SOMPROF: a vertically explicit soil organic matter model

Maarten C. Braakhekke[a,b,c,*], Christian Beer[a], Marcel R. Hoosbeek[b], Markus Reichstein[a], Bart Kruijt[b], Marion Schrumpf[a], Pavel Kabat[b]

[a] *Max Planck Institute for Biogeochemistry, P.O. Box 100164, 07701 Jena, Germany*
[b] *Wageningen University, Department of Environmental Sciences, Earth System Science and Climate Change Group, P.O. Box 47, 6700AA Wageningen, The Netherlands*
[c] *International Max Planck Research School on Earth System Modelling, Hamburg, Germany*

Abstract

Most current soil organic matter (SOM) models represent the soil as a bulk without specification of the vertical distribution of SOM in the soil profile. However, the vertical SOM profile may be of great importance for soil carbon cycling, both on short (hours to years) time scale, due to interactions with the soil temperature and moisture profile, as well as on long (years to centuries) time scale because of depth-specific stabilization mechanisms of organic matter. It is likely that a representation of the SOM profile and surface organic layers in SOM models can improve predictions of the response of land surface fluxes to climate and environmental variability. Although models capable of simulating the vertical SOM profile exist, these were generally not developed for large scale predictive simulations and do not adequately represent surface organic horizons. We present SOMPROF, a vertically explicit SOM model, designed for implementation into large scale ecosystem and land surface models. The model dynamically simulates the vertical SOM profile and organic layer stocks based on mechanistic representations of bioturbation, liquid phase transport of organic matter, and vertical distribution of root litter input. We tested the model based on data from an old growth deciduous forest (Hainich) in Germany, and performed a sensitivity analysis of the transport parameters, and the effects of the vertical SOM distribution on temporal variation of heterotrophic respiration. Model results compare well with measured organic carbon profiles and stocks. SOMPROF is able to simulate a wide range of SOM profiles, using parameter values that are realistic compared to those found in previous studies. Results of the sensitivity analysis show that the vertical SOM distribution strongly affects temporal variation of heterotrophic respiration due to interactions with the soil temperature and moisture profile.

Keywords: soil organic carbon model, vertical soil organic matter profile, surface organic layer, soil organic matter transport, bioturbation, dissolved organic matter transport

1. Introduction

Because soils globally store a huge amount of carbon, the response of soil carbon cycling to future climate change is currently subject to great attention (Trumbore and Czimczik, 2008; Heimann and Reichstein, 2008). Increasing temperatures will lead to accelerated heterotrophic respiration (Davidson and Janssens, 2006), while concurrently the increasing atmospheric CO_2 concentration is expected to cause higher vegetation productivity (Norby et al., 2005), resulting in greater soil carbon input. The present uncertainty with respect to the magnitude of these two mechanisms is demonstrated by the large disagreement of ecosystem models on future land surface CO_2 fluxes (Jones et al., 2003, 2005; Friedlingstein et al., 2006).

The focus of studies of soil carbon dynamics has classically been on the upper 20 to 50 cm of the soil (e.g., Jenkinson and Rayner, 1977; Gregorich et al., 1996). This layer (from hereon referred to as the "topsoil") is most directly influenced by climate, vegetation and land use, and generally contains much higher organic matter concentrations than the subsoil. Furthermore, the subsoil is below the rooting zone of most crops, while its organic matter appears to be stable on the time scale of anthropogenic climate change (Scharpenseel et al., 1989; Trumbore, 2000). Therefore, application of soil organic matter (SOM) models has focused on a bulk description of the organic matter in the topsoil, without specification of the vertical distribution. (Parton et al., 1987; Schimel et al., 1994).

Recently, interest in organic matter at greater soil depths has grown, mainly for two reasons. First, several recent studies have shown that the deep soil stores a considerable amount of carbon, which had previously not been included into estimates of global stocks (Batjes, 1996; Jobbagy and Jackson, 2000; Tarnocai et al., 2009).

Second, accumulating evidence contests the assumption that deep soil carbon is intrinsically stable. SOM can be stabilized by a myriad of mechanisms, many of which are reversible (von Lützow et al., 2006). Usually, different stabilization mechanisms are operating at different depths within a single soil profile. For example, Fontaine et al. (2007) found that energy limitation of microbes is more important as a stabilization mechanism in the subsoil than in topsoil, although these results were

*Corresponding author
Email address: Maarten.Braakhekke@bgc-jena.mpg.de (Maarten C. Braakhekke)

contradicted by Salomé et al. (2010) who found the reverse. Conversely, stabilization due to organo-mineral interactions is occurring in most of the soil profile, but increases in relative importance with depth (Rumpel et al., 2002).

Recent studies suggest that deep soil carbon may become destabilized under changing conditions, depending on the specific stabilization mechanism. For example, increased root exudation and root litter production, occurring under elevated CO_2 levels (Philips et al., 2006; Iversen, 2010) can lead to decomposition of old SOM due to priming of microbial activity (Drigo et al., 2008; Fontaine et al., 2007). Furthermore, it has been suggested that chemically recalcitrant SOM fractions are more sensitive to temperature increase (Conant et al., 2008; Davidson et al., 2006; Knorr et al., 2005), although this is under dispute (Fang et al., 2005; Reichstein et al., 2005). At the same time, physically protected SOM is likely less sensitive to warming, but more vulnerable to physical disturbance (Diochon and Kellman, 2009). Efforts are being made to include different stabilization mechanisms explicitly in SOM models in order to improve predictions of soil carbon cycling at decadal to centennial time scales (Wutzler and Reichstein, 2008; von Lützow et al., 2008; Manzoni and Porporato, 2009).

But also on short (hourly to annually) time scales the vertical distribution of organic matter plays an important role for soil carbon cycling. Soil properties usually show a strong depth gradient, with strongest temporal variations occurring near the surface. Respiration in surface layers usually responds more strongly to weather fluctuations, whereas subsoil respiration shows less temporal variation (Fierer et al., 2005; Hashimoto et al., 2007; Davidson et al., 2006). Hence, a soil with a deep organic matter distribution is likely to respond differently to short term weather fluctuations than a soil where most organic matter is stored near the surface. Because many factors are simultaneously, and often non-linearly, influencing decomposition rates, aggregating respiration over the profile in models may lead to incorrect results (Subke and Bahn, 2010).

Thus, an explicit representation of the vertical SOM distribution in biogeochemical models could significantly improve predictions of carbon cycling, as well as facilitate addition of new process descriptions. Such a model should include explicit representation of the processes leading to organic matter input at depth: root litter production and downward transport of organic matter. These models (referred to as "SOM profile models" from hereon) have already been proposed more than three decades ago (O'Brien and Stout, 1978; Nakane and Shinozaki, 1978). O'Brien and Stout (1978) applied a diffusion model of downward organic matter transport to explain carbon isotope profiles. Since then, various researchers have applied similar models, including diffusion or advection or both (Dörr and Münnich, 1989; Elzein and Balesdent, 1995; Baisden et al., 2002; Bosatta and Ågren, 1996; Bruun et al., 2007; Jenkinson and Coleman, 2008; Freier et al., 2010).

Most of these models, however, were developed to explain organic carbon and tracer profiles, not for predictive simulations of soil carbon cycling, and as such do not account for the influence of soil temperature and moisture on decomposition. A notable exception is the work of Jenkinson and Coleman (2008) who developed a vertically explicit version of the well-known SOM model RothC (Jenkinson, 1990), by adding two parameters: one that moves SOM down the profile in an advection-like manner, and another that slows decomposition with depth. Though innovative, their scheme was in fact a downward extrapolation of the original model, and is difficult to transfer to a different SOM model.

Furthermore, none of the published models include a representation of the surface organic layer. Consisting mostly of organic material, the organic layer has markedly different properties than the mineral soil, and behaves differently in terms of soil hydrology and heat transport. An explicit representation of this layer in the model would therefore be particularly valuable in the land surface scheme of a global climate model.

Despite past efforts to develop SOM profile models, the development of a general understanding of SOM profile formation has been slow, in part caused by the high complexity and the extremely slow rates of the relevant processes. An additional problem is posed by the lack of a standardized approach to determine transport rates with inverse modelling. The assumptions inherent to the model structure used in parameter estimation strongly influence the final parameter estimates (Bruun et al., 2007). For example, failure to include a relevant mechanism for subsoil organic matter input will inevitably lead to under- or overestimation of the importance of other processes. The diversity of the models in the published studies is such that the usefulness of direct comparison of transport rates is questionable.

Taken that the ultimate aim is to develop a SOM profile model that can be applied for global simulations, there is a need for a standardized and mechanistic scheme for modelling SOM transport to allow transfer of parameters between models. On the other hand, such a scheme should be parsimonious enough to allow development of a large scale parameter set. The model presented here, SOMPROF, has been developed with these considerations in mind. SOMPROF is based on earlier SOM profile models, with several important additions, including explicit representation of surface organic horizons and the effects of soil temperature and moisture on decomposition. Rather than lumping all SOM transport processes into either a diffusion or an advection term, explicit distinction is made between bioturbation and liquid phase transport. In this paper we present the model and its underlying rationale. Furthermore, we test the sensitivity to the input parameters, and study the effects of the vertical SOM distribution on predicted heterotrophic respiration.

2. Theory and model description

We will not give an exhaustive description of SOMPROF here, but instead focus on the parts that are innovative compared to existing SOM models and discuss the rationale behind the model structure. Particular attention is given to the reasoning behind the implementation of the transport processes. A full description, including all model equations, can be found in Appendix A.

In the following description, depth is denoted with z (m) and time with t (yr). Depth is assumed positive downwards and

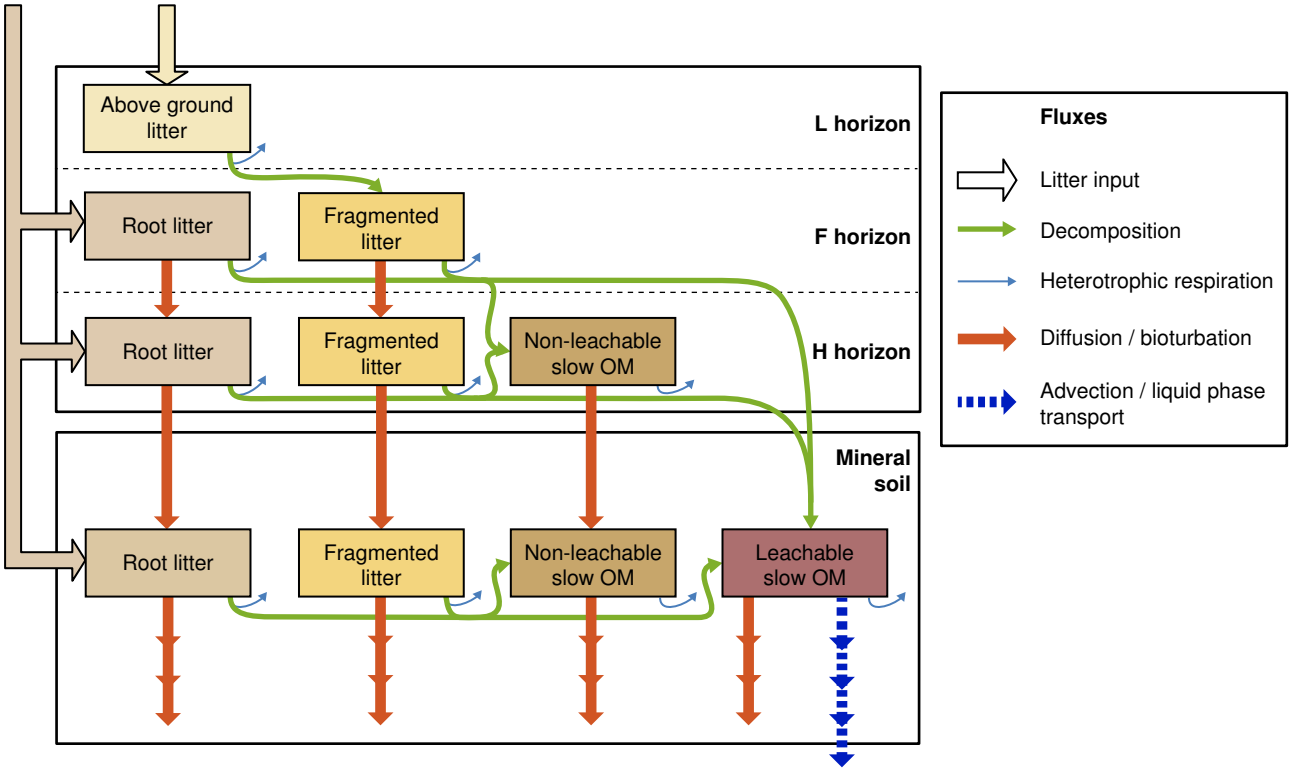

Figure 1: Overview of the SOMPROF model

$z = 0$ is set at the top of the mineral soil. Organic matter (OM) quantity C is simulated in the mineral soil as concentrations (kg m^{-3}), and in the organic horizons (L, F and H) as stocks (kg m^{-2}).

2.1. *General structure*

A mechanistic model of the vertical soil organic matter profile must consider the vertical distribution of root litter input and downward organic matter transport processes (Lorenz and Lal, 2005). The mathematical description of vertical transport processes usually comprises terms for diffusion, advection, or both. However, such a scheme is unsuitable for the organic layer. Transport models typically simulate concentrations as unit mass per unit volume. This concentration is only a valid quantity in the context of a mixture consisting of several materials. In the mineral soil, where organic matter is mixed with minerals material, this approach is justified, but in the organic layer, where the organic matter concentration far exceeds the mineral concentration, the organic matter itself forms the bulk and the organic matter concentration becomes an undefined quantity. The vertical distribution of properties such as organic matter quality and element concentrations is therefore dominated by organic matter input and loss due to litter deposition and decomposition, and cannot be explained by vertical mixing alone. This problem was demonstrated by Kaste et al. (2007) who found that a transport model could well explain the vertical profile of the radioactive lead isotope ^{210}Pb in the mineral soil but not in a thick organic layer. Instead, a model that ignored vertical transport due to mixing and accounted for the effects of litter accumulation and decomposition proved more able to reproduce the observed ^{210}Pb profile.

Hence, in SOMPROF the diffusion-advection model is not applied to the organic layer. The organic layer is explicitly split into three layers: the L, F and H horizon[1] (figure 1). The organic horizons are simulated as separate, homogenous reservoirs of organic matter. When organic matter in one layer is transformed to more decomposed material, it flows to the underlying layer. This represents the process of continuous burial and decomposition that occurs in the organic layer and leads to the formation of a vertical gradient of decomposition stage that is typically observed in the field (van Delft et al., 2006). Bioturbation reduces this gradient by causing downward flow from the F to the H horizon and from the H horizon to the mineral soil. Because we assume that the material in the L horizon is not transported, this horizon is always present if above ground litter input occurs. On the other hand, the F and H horizon may be absent if the bioturbation rate exceeds the input of material. Liquid phase transport (advection) within the organic layer is not explicitly considered; we assume that all material that can be transported with the liquid phase immediately flows to the mineral soil.

In the mineral soil, the organic carbon concentration as a function of depth is simulated using a transport model includ-

[1]These horizon codes are used to designate organic horizons in several soil classification systems (Soil Classification Working Group, 1998; van Delft et al., 2006) and approximately correspond the Oi, Oe and Oa horizon in the U.S. (Soil Survey Division Staff, 1993) and FAO (IUSS Working Group WRB, 2007) systems.

ing diffusion, representing bioturbation, and advection, representing liquid phase transport. Currently, the model does not account for the presence of stones in the mineral soil matrix.

2.2. Organic matter pools

SOMPROF follows the classical organic matter pool approach with five types of organic matter (table 1). The organic matter pools are chosen to represent functionally different types of organic matter that differ with respect to decomposition rate and transport behavior. The pools have a serial arrangement: upon decomposition material flows from less to more decomposed pools. This setup was chosen rather than parallel pool arrangement to be able to represent the change of transport behavior when organic matter is transformed.

Above ground litter. Above ground litter is material accumulating at the surface and is easily decomposable. Since this is typically coarse material, we assume that it is not transported and is therefore only present in the L horizon. No distinction is made between different types of litter (e.g. leaves, woody debris).

Fragmented litter. In the first decomposition step, above ground litter is transformed to fragmented litter which flows immediately to the F horizon, thus forming the most important organic matter fraction of this layer. This transformation represents early litter decomposition during which material is fragmented. Fragmented litter is assumed to be chemically similar to above ground litter and has a relatively high decomposition rate. However, contrary to above ground litter, fragmented litter can be transported by bioturbation, which thus acts as a mechanism for the introduction of easily degradable material in the H horizon and mineral soil.

Root litter. Root turnover provides input for the root litter pool in the mineral soil and the F and H horizon. We assume root growth, and thus root turnover, to be negligible in the L horizon. Since root litter is largely produced by the turnover of fine roots, we assume that it is chemically similar to above ground litter. But, contrary to above ground litter, it can be transported by bioturbation. The total root litter production rate is specified as model input and vertically distributed according to an exponentially decreasing function of depth, which starts at the top of the F horizon. The root litter input into a given layer is obtained by integrating the distribution function over the layer thickness.

Non-leachable slow organic matter. Part of the decomposition products of the fragmented litter and root litter pools flow into the non-leachable slow (NLS) organic matter pool. Non-leachable slow OM comprises chemically stabilized particulate organic matter and forms the basis of the H horizon. It is formed in the organic layer and in the mineral soil and can be transported by bioturbation. Non-leachable slow OM formed from litter in the in the F horizon flows immediately into the H horizon, while NLS-OM formed in the H horizon stays there, although it may subsequently be transported into the mineral soil by bioturbation.

Leachable slow organic matter. The leachable slow (LS) organic matter pool represents organic matter adsorbed to the mineral phase. Since this material can enter the liquid phase through desorption, it is transported by advection as well as bioturbation. Hence, liquid phase transport is included in SOMPROF, even though dissolved organic matter is not explicitly represented. The rationale behind this approach is discussed in section 2.4.2. Organic matter adsorption onto the mineral phase is typically very strong and protects organic matter against decomposition, hence the LS organic matter pool is presumably the most stabilized type of organic matter in the model.

2.3. Organic matter decomposition

Decomposition of organic matter is simulated according to first order kinetics using a base decomposition rate which is corrected for soil temperature and moisture using response factors (Appendix A.1). A first order decomposition rate k at reference temperature (10 °C) and optimal soil moisture is specified for each organic matter pool as part of the model input. For the response of decomposition to soil temperature we use the modified Arrhenius function from Lloyd and Taylor (1994), in which the temperature sensitivity decreases with increasing temperature. Response to soil moisture is defined according to a sigmoid function from Subke et al. (2003). Measured or modeled depth profiles of temperature and moisture are input, hence the decomposition response factors are depth dependent. If necessary, the profiles are interpolated to the midpoint depths of the organic horizons and the soil layers used for numeral solution (section 2.6).

As discussed in section 2.2, several pools are transformed to other pools during decomposition. The transformation fluxes are determined by a transformation factor α (-) that specifies how much of the decomposition flux of donor pool flows to the receiving pool. The material that does not flow to another pool ($1 - \sum_j \alpha_{i \to j}$) is assumed to be lost as CO_2, representing heterotrophic respiration. Note that all transformation factors other than those for the decomposition of the above ground litter, root litter and fragmented litter are zero.

Contrary to some other models, the decomposition rates are not explicitly reduced with depth in SOMPROF. Elzein and Balesdent (1995) showed that with a multi-pool organic matter model, the assumption of explicitly decreasing turnover rates with depth is not required to reproduce ^{14}C profiles because the change of apparent turnover time with depth emerges from the change of relative distribution of the organic matter pools. Depth specific stabilization mechanisms are currently not yet fully understood, hence, in view of parsimony we do not include these processes at this stage of model development.

2.4. Organic matter transport

SOMPROF includes two organic matter transport processes: bioturbation and liquid phase transport. Other transport processes are known to occur in certain soils, such as mixing due to freezing and thawing (cryoturbation) and mixing due to shrinking and swelling. Although locally these processes may be very

Table 1: The organic matter pools in SOMPROF

	Decomposition rate	Source	Diffusion	Advection
Above ground litter (AGL)	high	external input into L horizon	no	no
Fragmented litter (FL)	intermediate	formed from Above ground litter	yes	no
Root litter (RL)	high	external input into F, H and mineral soil	yes	no
Non-leachable slow OM (NLS)	low	formed from fragmented and root litter	yes	no
Leachable slow OM (LS)	low	formed from fragmented and root litter	yes	yes

important, they occur only under specific conditions. In general bioturbation and liquid phase transport can be assumed to be the dominant transport mechanisms in most soils, hence other transport processes are not explicitly considered (although they may be implicitly included, depending on how the transport parameters are estimated).

Except for the influence of bulk density on the diffusivity (see below), the transport rates are kept constant with depth. In reality this is probably not the case since the soil fauna biomass decreases with depth, and water fluxes and adsorption of dissolved organic matter are likely depth dependent as well. However, past studies have shown that SOM and tracer profiles can be well reproduced using constant transport rates (Dörr and Münnich, 1989; Elzein and Balesdent, 1995; Bruun et al., 2007; Jenkinson and Coleman, 2008). On the other hand, making the transport parameters depth dependent introduces additional degrees of freedom which complicates parameter estimation based on measurements.

2.4.1. Bioturbation

Bioturbation refers to the reworking of soil by soil animals and to a lesser degree by plants (Meysman et al., 2006). The activities of these organisms mix the soil matrix, representing an important mechanism for organic matter flow within the organic layer and mineral soil (Hoosbeek and Scarascia-Mugnozza, 2009; Tonneijck and Jongmans, 2008). Estimates of soil fauna mixing activity are typically expressed as reworking rates, the amount of material moved per unit surface area (Wilkinson et al., 2009). For example, earthworm activity at the population level is often estimated by measuring rates of surface cast deposition. (See Paton et al., 1995, for a comprehensive overview of many bioturbation rate esimates for different animal species and plants.)

In general, bioturbation causes homogenization of soil properties, i.e. net transport of soil constituents inversely proportional to the concentration gradient. Therefore, the effects of bioturbation on the distribution of soil properties has often been modeled using Ficks diffusion equation (Elzein and Balesdent, 1995; van Dam et al., 1997; Kaste et al., 2007). Using mixing length theory developed for turbulent mixing in gasses and fluids, it can be shown that bioturbation can indeed lead to diffusive behavior of soil constituents (Boudreau, 1986, Appendix B). However, the validity of the diffusion model for stochastic mixing processes such as bioturbation is not self-evident but depends on several criteria. (These have been thoroughly discussed in the context of benthic bioturbation: Boudreau, 1986; Meysman et al., 2003). Most important, (i) the time between mixing events must be short compared to other processes that influence the concentration profile; (ii) the length scale of the mixing (the distance over which soil particles are moved) must be small compared the scale of the concentration profile and; (iii) the mixing should be isotropic, i.e. equal in both up and down direction.

At small spatial scales ($\sim 1\,\mathrm{m}^{-2}$) bioturbation cannot be expected to meet these criteria. Mixing of soil particles occurs as sudden jumps followed by long periods of rest, hence the local instantaneous concentration of any soil constituent depends strongly on whether or not a mixing event has recently occurred, particularly if mixing is done by larger organisms (e.g. burrowing mammals, uprooted trees).

However, for describing the average transport of many mixing events the diffusion model can be assumed to be valid. Such averaging may be over time, if the mixing is stationary, or over space if the mixing is homogenous (Hinze, 1975, p.5). The latter suggests that at sufficiently large spatial scales within a single ecosystem, the assumption of diffusive behavior is reasonable. Hence, we assume that the diffusion approach is valid at ecosystem scale, for which SOMPROF is designed. Vertical transport due to bioturbation in the mineral soil is defined as:

$$\left.\frac{\partial C_i}{\partial t}\right|_{\mathrm{BT}} = D_{\mathrm{BT}} \frac{\partial^2 C_i}{\partial z^2} \,. \tag{1}$$

where C_i is the organic matter concentration of pool i (kg m^{-3}) and D_{BT} is the diffusivity due to bioturbation (m^2 yr^{-1}). All organic matter pools are assumed to be transported equally according to (1), except for the above ground litter pool, which is not transported (section 2.2). At the top of the mineral soil, a flux prescribed boundary condition is used, which is determined by the bioturbation rate (see below). At the bottom of the soil profile, a zero-gradient boundary condition is used, which means that no material is transported by bioturbation over the lower boundary.

Since the diffusive behavior of organic matter is the direct result of the mixing activity of the soil fauna, there must be a unique relationship between the diffusivity D_{BT} and the bioturbation rate B (kg m^{-2} yr^{-1}). Continuing the mixing length analogy, it can be shown that the diffusivity is composed of the time-averaged correlation between the fluctuation of the vertical advection rate of transported material and the distance over which the material is moved (Boudreau, 1986, Appendix B). The fluctuation of the vertical advection rate is directly related to the bioturbation rate via the bulk density ρ^{MS} (kg m^{-3}). Fur-

thermore, we assume that there exists a typical distance over which material is moved by the soil fauna, the mixing length l_m (m) which must be determined later. The diffusion can then be estimated from the bioturbation rate as follows:

$$D_{\mathrm{BT}} = \frac{1}{2}\frac{B}{\rho^{\mathrm{MS}}} l_m \,. \tag{2}$$

Note that B refers only the *vertical* component of the mixing. If the bioturbation rate is estimated from ingestion rates of earthworms, it must be multiplied by an additional factor of 0.5 to obtain the mixing rate in the vertical direction (Wheatcroft et al., 1990). Measurements of earthworm cast formation can be assumed to represent vertical mixing only. As said, the diffusion model represents the effective transport behavior of SOM averaged over long time scales and large areas. As such, equations (1) and (2) should not be viewed as a mechanistic description of the mixing activity of the soil fauna, nor is the mixing length parameter a physical quantity that can be measured. Rather, mixing length theory provides justification for a simple linear empirical relationship between the diffusivity and the soil fauna activity. More specifically, in SOMPROF l_m is used as a tuning parameter that links the bioturbation fluxes within the organic layer (see below) to the transport within the mineral soil.

The bulk density ρ^{MS} can either be specified or estimated (section 2.5). From (2) it follows that the diffusivity due to bioturbation is inversely proportional to bulk density. This is consistent with our rationale: the diffusivity is limited only by the capacity of the soil fauna to displace a certain amount of mass per unit time, not by the volume over which this mass is distributed. Hence, the diffusion coefficient must increase with decreasing bulk density to maintain the same rate of mass transport.

For reasons discussed in section 2.1, the diffusion model is not applied to the organic surface horizons. Instead, we assume that the total net flux of organic matter from F to H and from H to the mineral soil is equal to the bioturbation rate B (Appendix A.4). We do not consider upward transport of mineral material from the mineral soil to the organic layer. If the mass of a layer is zero, the flux is set to the total input minus the loss from decomposition in this layer, to avoid that the mass becomes negative. The flux from H to mineral soil serves as the upper boundary flux for the transport scheme of the mineral soil.

2.4.2. Liquid phase transport

Liquid phase transport refers to the combined effects of formation, transport, and ad- and desorption of dissolved organic matter (DOM). Although DOM concentrations are usually very small compared to immobile organic matter, transport in the liquid phase represents a major contribution to downward organic matter movement, particularly in soils with little biological activity (Kalbitz and Kaiser, 2008). DOM, once formed, flows down with infiltrating water and may be reversibly adsorbed to mineral particles upon which it becomes immobile (Kalbitz et al., 2000).

Models of short time scale DOM dynamics have been applied with some success at site scale (e.g. Neff and Asner, 2001; Michalzik et al., 2003). However, DOM fluxes in the field are notoriously difficult to predict due to spatial heterogeneity of mineral composition and DOM chemistry—which determine DOM adsorption behavior—and water infiltration, which is often dominated by macropore flow and storm events (Kalbitz et al., 2000). Consequently, simulation of long time scale SOM profile evolution based on a mechanistic description of DOM transport and adsorption is not feasible. Furthermore, simulation of DOM transport requires accurate simulation of water fluxes at short (sub-daily) time scales, while SOMPROF is designed to be run with daily or longer time steps.

Therefore, downward movement of organic matter as DOM is not modeled explicitly. We define a pool that can potentially enter the liquid phase and be transported downward advectively: leachable slow (LS) organic matter, which is equivalent to the reactive soil pool, introduced by Nodvin et al. (1986). Downward movement with the liquid phase is simulated by defining an effective advection rate v (m yr^{-1}):

$$\left.\frac{\partial C_{\mathrm{LS}}}{\partial t}\right|_{\mathrm{adv}} = -v\,\frac{\partial C_{\mathrm{LS}}}{\partial z} \,. \tag{3}$$

This scheme is similar to the retardation factor approach, which has been successfully applied in studies of transport of tracers and pollutants in soils (e.g. Huang et al., 1995). This method simulates both the adsorbed and dissolved fraction as one pool by correcting the transport rate of the dissolved fraction with the retardation factor, which accounts for interactions with the solid phase. The underlying assumptions of the retardation factor approach are that the adsorption isotherm is linear, and that the dissolved and adsorbed fraction are locally in equilibrium with each other. When these conditions hold, the relative distribution of the studied compound over the dissolved and adsorbed fraction is fixed and independent of the concentration in the liquid phase. Several of the published DOM models are based on the same assumptions (Jardine et al., 1989; Michalzik et al., 2003).

In SOMPROF, the retardation factor concept is expanded to organic matter decomposition: the breakdown of organic matter is retarded by adsorption to the mineral phase. Hence, the decomposition rate of LS organic matter is also an effective parameter for both fractions. However, in practice the influence of the dissolved fraction on the effective decomposition rate and total carbon concentration will be negligible since adsorbed organic matter is present in much higher quantities than DOM. Hence, we do not consider the dissolved fraction when comparing with measurements. Note that the LS-OM pool is also transported by bioturbation. The upper boundary condition of (3) is comprised of the combined production of LS-OM in the organic layer.

SOMPROF differs from other SOM profile models (e.g. Elzein and Balesdent, 1995) in that only a specific pool is moved advectively, rather than all organic matter. Although this introduces additional model parameters, it is clearly closer to reality since not all organic matter can be transported with the liquid phase. Furthermore, the fraction of organic matter that is potentially mobile presumably increases with depth, since liquid phase transport reaches greater depths than bioturbation and

root litter input.

Contrary to bioturbation, liquid phase transport may lead to a loss of organic matter from the system. For a given soil, this depends on the depth at which the lower boundary is set. If it is set shallow enough that the bottom LS-OM concentration is significantly higher than zero, organic matter is lost and is not included in the calculation of organic matter stocks and heterotrophic respiration.

In the organic layer the adsorptive capacity of the solid phase is negligible compared to that in the mineral soil, due to the absence of the mineral material. Therefore, we assume that all LS-OM produced in the organic layer immediately flows into the mineral soil and that the concentration of LS-OM in the organic layer is zero.

2.5. Bulk density

The thickness of the organic horizons is estimated from their mass using the bulk density, which is specified as model input separately for the L, F and H horizons (ρ^{L}, ρ^{F}, ρ^{H}). The bulk density in the mineral soil ρ^{MS} is required to convert the mass-based bioturbation rate to the volume-based diffusivity (section 2.4.1). Furthermore, the bulk density profile affects the shape of the organic matter profile. Bulk density is usually strongly correlated with soil organic matter content. If measurements are not available, SOMPROF estimates bulk density from the soil organic matter fraction using an equation proposed by Federer et al. (1993). These authors proposed that the soil is a hypothetical mixture of pure mineral material and pure organic material, that both have a bulk density. Assuming that their bulk densities mix linearly, the bulk density of the mixture is estimated as:

$$\rho^{\mathrm{MS}} = \frac{\rho_{\mathrm{M}}\rho_{\mathrm{O}}}{f_{\mathrm{O}}^{\mathrm{MS}}\rho_{\mathrm{M}} + (1 - f_{\mathrm{O}}^{\mathrm{MS}})\,\rho_{\mathrm{O}}}\,, \tag{4}$$

where ρ_{M} and ρ_{O} are the bulk densities of the mineral and organic fractions, respectively (kg m^{-3}), and f_{O} is the organic matter fraction (-). ρ_{O} is set equal to the bulk density of the H horizon.

2.6. Model solution and simulation setup

SOMPROF is solved for discrete time steps using standard finite differencing techniques. The model compartments are solved in order from top to bottom: L, F, H, mineral soil. For the organic horizons, first the pools are updated for input and decomposition, using an explicit scheme. Next it is determined whether the maximum bioturbation flux can be met, and if necessary it is adjusted downward. Then the mineral soil is updated using a fully implicit scheme with upwind differencing for advection. To this end, the soil is split into compartments of variable thickness. The compartment thicknesses as well as the depth of the lower boundary can be chosen freely, depending on the available computational resources and the desired resolution of the model output. For the simulations discussed in section 3, we used 11 compartments, with thicknesses increasing from 0.5 cm at the surface to 50 cm at the bottom of the profile.

Near the soil surface, the concentration of organic matter may be high enough that its mass is no longer negligible compared to that of the matrix. Therefore, the compartment thicknesses are corrected for change of mass at every time step, once the new concentrations of organic matter are known (Appendix A.4).

To avoid aggregation errors due to the non-linearity of the soil temperature and moisture response function (Appendix A.1), the response factors are calculated before the model run, at the temporal resolution at which they are available (typically at half hourly intervals). These response factors are then averaged to the time step length of the model and used as input. Since the compartments thicknesses change during the simulation, the response factors as well as measured bulk densities (if available) are interpolated at every time step using piecewise cubic Hermite interpolation to obtain values at the midpoint depths of the compartments and organic horizons.

A typical model run consists of two stages: (i) a spin-up stage, starting from bare ground, i.e. without organic matter, during which the model is run with an average annual cycle of soil moisture, soil temperature and litter fall; and (ii) the actual simulation for which measurements of soil temperature, moisture and litter fall are available. The purpose of the spin-up stage is to obtain the initial conditions used for the second stage. The length of the spin-up period can be chosen freely and, in principle, should be the time since the start of the development of the organic matter profile. For many soils it may be acceptable to run the model in spin-up until the slowest carbon pools and the vertical distribution are in equilibrium (~1000 years).

2.7. Model input

Almost all input data required to run SOMPROF (table 2) depends strongly on soil and ecosystem type. Several of these quantities can be measured directly in the field, including the above ground and below ground litter production, the soil temperature and moisture and the root (litter input) distribution profile. In a biogeochemical model, these parameters can be supplied by other submodels (e.g. vegetation or land surface models), or derived from the vegetation and soil type.

2.7.1. Decomposition parameters

The parameters of the decomposition submodel include the decomposition rates k at reference temperature (10 °C) and the transformation factors α. The three litter pools (above ground litter, fragmented litter and root litter) are chemically similar in the sense that they have a relatively high decomposition rate. Typical values range from 0.1 to 1 yr^{-1} (Paustian et al., 1997; Berg and McClaugherty, 2003). The non-leachable and leachable slow organic matter pools represent stabilized fractions. It is likely that the LS-OM pool is the more recalcitrant of the two, since this pool consists largely of organic matter adsorbed to the mineral phase, which is thought to be very stable (von Lützow et al., 2006; Kaiser and Guggenberger, 2000). Since the LS-OM pool reaches deeper layers than the other pools, the decomposition rate of this fraction should correspond to organic carbon ages and turnover times found in the deep soil,

Table 2: List of model input required to run SOMPROF and values used for the reference simulation

Parameter	Symbol	Units and value in reference simulation
Litter input		
Above ground litter input*	$I^{\mathrm{L}}_{\mathrm{AGL}}$	0.314 kgC m^{-2} yr^{-1} †
Total annual root litter input*	$I^{\mathrm{tot}}_{\mathrm{RL}}$	0.178 kgC m^{-2} yr^{-1} †
Root litter distribution parameter	β	0.07 m^{-1}
Decomposition		
Above ground litter decomposition rate	k_{AGL}	0.5 yr^{-1}
Root litter decomposition rate	k_{RL}	0.5 yr^{-1}
Fragmented litter decomposition rate	k_{FL}	0.2 yr^{-1}
Non-leachable slow OM decomposition rate	k_{NLS}	0.05 yr^{-1}
Leachable slow OM decomposition rate	k_{LS}	0.005 yr^{-1}
Above ground litter - fragmented litter transformation factor	$\alpha_{\mathrm{AGL}\to\mathrm{FL}}$	0.8
Fragmented litter - NLS transformation factor	$\alpha_{\mathrm{FL}\to\mathrm{NLS}}$	0.15
Fragmented litter - LS transformation factor	$\alpha_{\mathrm{FL}\to\mathrm{LS}}$	0.15
Root litter - NLS transformation factor	$\alpha_{\mathrm{RL}\to\mathrm{NLS}}$	0.15
Root litter - LS transformation factor	$\alpha_{\mathrm{RL}\to\mathrm{LS}}$	0.15
Soil temperature response parameter	E_a	308.56 K
Soil moisture response parameter	a	1
Soil moisture response parameter	b	20
Soil temperature*	T	K
Relative soil moisture content*	M	-
Organic matter transport		
Bioturbation rate	B	0.4 kg m^{-2} yr^{-1}
Mixing length	l_m	0.3 m
Advection rate	v	0.002 m yr^{-1}
Bulk density		
Bulk density L layer	ρ^{L}	50 kg m^{-3}
Bulk density F layer	ρ^{F}	100 kg m^{-3}
Bulk density H layer‡	ρ^{H}	150 kg m^{-3}
Bulk density mineral soil*	ρ^{MS}	kg m^{-3}
Mineral bulk density§	ρ_{M}	kg m^{-3}
Other input		
Spin-up length	-	1000 yr
Depth of bottom boundary	L	0.7 m

* Time and/or depth dependent
† Average annual value for the spin-up
‡ ρ^{H} is also used as the organic bulk density ρ_{O} for determining ρ^{MS} (section 2.5).
§ Not required if ρ^{MS} is specified

i.e. 10^{-3} to 10^{-2} yr^{-1}. The non-leachable slow pool represents organic matter stabilized by other mechanisms (e.g. chemical recalcitrance or spatial inaccessibility), and is assumed to have a decomposition rate between 10^{-1} and 10^{-2} yr^{-1}.

The transformation factors determine the flow between the organic matter pools and lie between 0 and 1 . Since these parameters are rather abstract, they are more difficult to predict a priori, but we can gain some insight from parameterizations of other decomposition models with a similar structure (e.g. van Dam et al., 1997; Elzein and Balesdent, 1995). In these models, the efficiency of the decomposition usually increases with successive decomposition steps, meaning that a greater fraction of the organic matter is metabolized. It is likely that little material is lost during the transformation of above ground litter to fragmented litter, hence we expect $\alpha_{\mathrm{AGL}\rightarrow\mathrm{FL}}$ to be in the higher end of the range, 0.6 to 0.9 . The transformation factors for production of leachable and non-leachable slow OM ($\alpha_{\mathrm{FL}\rightarrow\mathrm{NLS}}$, $\alpha_{\mathrm{FL}\rightarrow\mathrm{LS}}$, $\alpha_{\mathrm{RL}\rightarrow\mathrm{NLS}}$, $\alpha_{\mathrm{RL}\rightarrow\mathrm{LS}}$) are presumably closer to zero: 0.05 to 0.4 .

The parameters of the temperature and moisture response factors can be found in literature if local measurements are not available (e.g. Lloyd and Taylor, 1994; Subke et al., 2003).

2.7.2. Transport parameters

Compared to decomposition, relatively little research has been done with respect to organic matter transport. The bioturbation rate B is determined by the soil fauna biomass and activity, which in turn strongly depends on soil and vegetation type and climate. Under inhospitable conditions for soil animals the mixing rate may be virtually zero, whereas very high mixing rates can be found for e.g. tropical soils. Paton et al. (1995) compiled an extensive list of estimates of reworking rates for different types of organisms and climates and found that earthworms are generally the most important organisms for bioturbation. Reported reworking ranged from 0.0063 to 27 kg m^{-2} yr^{-1}, with two thirds of the rates between 0 and 5 kg m^{-2} yr^{-1}. Since most of these estimates were rates of surface cast formation, they noted that these numbers are probably underestimations, since not all species deposit casts at the surface.

The mixing length l_m should ideally represent the typical distance over which soil particles are displaced. However, as discussed in section 2.4.1, in SOMPROF this parameter is of a more empirical nature. Nevertheless, we can expect the mixing length to be roughly in the order of magnitude of the body size of the soil fauna, i.e. 0.01 to 0.5 m. Ideally, this parameter should be relatively constant over different ecosystems.

The advection rate v is determined both by downward water fluxes and adsorption of DOM to mineral surfaces. Since SOMPROF differs from most other models in the sense that only part of the organic matter is transported advectively, little a priori information on this parameter is available. Sanderman et al. (2008) estimated effective DOM advection rates for the total organic matter fraction as a function of depth, based on field concentration measurements and modelled water fluxes. Assuming that in the deep soil most organic material is potentially mobile, their estimate of the effective advection rate for this fraction is approximately 0.2 mm yr^{-1}. Bruun et al. (2007) estimated transport rates from ^{14}C profile, and found an advection rate of 2.3 mm yr^{-1} for a fraction of 24 % of the total organic matter. Based on profiles of short-lived isotopes (^{137}Ce and ^{241}Am) produced by nuclear weapon testing, Kaste et al. (2007) reported advection rates ranging from 0.7 to 2 mm yr^{-1}, for different soils.

2.7.3. Bulk density

The bulk densities of the organic layers (ρ^{L}, ρ^{F} and ρ^{H}) are not usually measured in field studies. Since they are needed only to calculate the thickness of the organic layers in order to distribute the root litter input and soil temperature and moisture profiles, their influence on the carbon stocks and distribution is relatively small. For soil carbon cycling simulations they may be set to fixed but reasonable values (table 2). However, for energy and water exchange the bulk density of the organic horizons is more important, due to the effects of the organic layer on soil heat and moisture transport.

If the bulk density of the mineral soil (ρ^{MS}) is not available, it is estimated according to equation (4). In this equation, the organic bulk density ρ_{O} is set equal to the H horizon bulk density. The mineral bulk density depends on the mineral composition, and should be approximately equal to the bulk density at the deep soil, where the organic matter fraction approaches zero.

3. Simulation preparation

To test the model, a simulation was made using data from Hainich, a deciduous forest in Germany. Predicted soil carbon fractions and stocks are compared to measurements made at the site. However, we did not perform calibration the model parameters to these measurements, which, due to the complexity of the model, is outside of the scope of this paper. The organic carbon measurements are presented for reference, but we do not present any statistics on model performance.

To study the model behavior we prepared several additional simulations for which one or more parameters were changed. This section describes the preparation of the reference simulation. For each additional simulation, the changes with respect to the reference simulation are described in section 3.

3.1. Site description

Hainich is an old growth deciduous forest in Central Germany (51°4′45.36″N; 10°27′7.20″E) which has been unmanaged for several decades. The climate is temperate suboceanic/subcontinental with an average annual precipitation of 800 mm and an average temperature of 7 to 8 °C. The forest is dominated by beech (*Fagus Sylvatica*, 65 %) and Ash (*Fraxinus excelsior*, 25 %), with a wide range of age classes, up to 250 years. The understorey consists of herbaceous vegetation (*Allium ursinum*, *Mercurialis perennis*, *Anemone nemorosa*) which seasonally completely covers the forest floor (Kutsch et al., 2010).

The soil is classified as Luvisol or Cambisol (IUSS Working Group WRB, 2007; Kutsch et al., 2010) and consists of weathered limestone overlain by a Pleistocene loess layer of varying thickness (10–50 cm). The mineral soil is characterized by

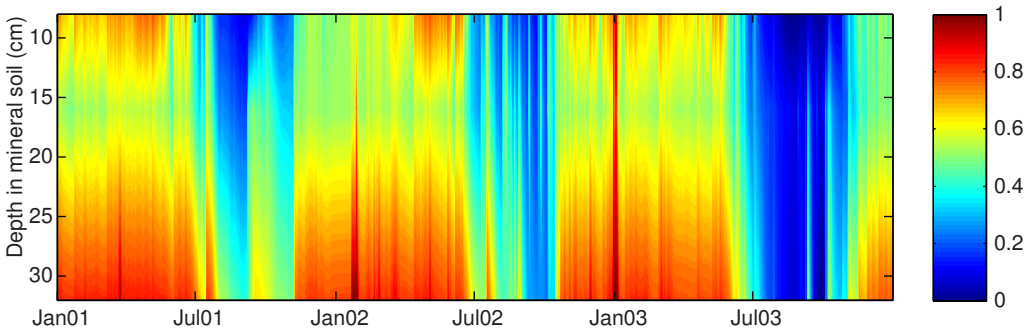

Figure 2: Measured relative soil moisture content at Hainich for the period 2001–2003 . Measurement depths were 8, 16 and 32 cm.

a high clay content (60 %) and a pH-H_2O of 6.0 to 7.8 (Søe and Buchmann, 2005). About 90 % of the root biomass occurs above 40 cm depth. The pH and litter quality of deciduous trees in Hainich support a high soil biological activity, demonstrated by a thin organic layer and a well developed A horizon of (10 to 15 cm; Søe and Buchmann, 2005). Cesarz et al. (2007) reported earthworm populations of up to 500 individuals per m^2 for the Hainich forest.

The high clay content and shallow bedrock at Hainich obstruct drainage, which causes the deep soil to be relatively moist throughout the year (figure 2).

3.2. Measurements and data processing

10 soil cores to a maximum depth of 70 cm were extracted in March 2004. Organic carbon fraction, root biomass and bulk density of the fine soil fraction were determined for 7 depth increments (0–5 cm; 5–10 cm; 10–20 cm; 20–30 cm; 30–40 cm; 50–60 cm; 60–70 cm). Organic carbon stocks were measured for L and F/H horizons (the individual F and H horizons could not be identified). The mineral soil organic carbon stocks were derived from the organic carbon fraction using the fine soil bulk density. The sampling and measurement procedures are described in Schrumpf et al. (2011).

Soil temperature and moisture were continuously measured at half-hourly intervals for the period 2001 to 2008. Gaps were filled with piecewise Hermite interpolation. Soil temperature was measured for two profiles at 5 depths (2, 5, 15, 30 and 50 cm). The average of the two soil temperature profiles was used for model input. Soil moisture was measured for one profile (8, 16 and 32 cm; figure 2). The soil moisture volume fraction was converted to relative content by calculating the relative value between the minimum value and the maximum value of the time series for each depth. Next, the half-hourly temperature and relative soil moisture content values were converted to response factors based on the response equations (Appendix A.1), and were subsequently averaged to daily values for the second stage of the simulation. Also, an average annual cycle of monthly values was derived for the spin-up.

Total annual litter fall and root litter production rate was measured for the period 2000 to 2007 (Kutsch et al., 2010). Average values for this period were used for the spin-up.

3.3. Simulation setup

For the reference simulation, the decomposition and transport parameters (table 2) were manually tuned based on a priori knowledge of the parameters (section 2.7) and model behavior.

During the spin-up phase, the model was run for a period of time to achieve the initial conditions for the second stage of the simulation. Although the oldest trees at Hainich are about 250 years old, development of the soil organic matter profile presumably started much earlier. Therefore, we used a spin-up length of 1000 years, during which the soil effectively reached an equilibrium. During the spin-up, the model was run at a monthly time step, and driven by an average annual cycle of soil temperature and moisture response factors, derived from the available measurements. Also, average annual values for above ground litter fall and root litter production were used during the spin-up (but the above ground litter fall is distributed over the year, see below).

During the second stage of the simulation, SOMPROF was run at a daily time step for the period 2001 to 2007, and driven by local measurements of soil temperature, moisture and above and below ground litter production. Since no local estimates of the soil moisture and temperature sensitivity are available, the parameter values from Lloyd and Taylor (1994) were used for the temperature response function. The parameters of the soil moisture response were chosen such that respiration starts to decrease sharply when relative soil moisture drops below 20 %. To account for seasonal variations, the annual total above ground litter fall was distributed over the year (for the spin-up as well as the second phase of the simulation) according to a distribution function based on data for a similar forest, taken from Lebret et al. (2001). Since no information about the seasonal cycle of root litter production was available, it was kept at a constant rate throughout the year. An exponential function was fitted to the vertical root biomass profile to determine the vertical distribution of root litter input.

The subsoil at Hainich has a high stone content which increases towards the bedrock. Since SOMPROF does not account for stones, the fine soil density (mass of grains smaller than 2 mm per unit total volume) was used as bulk density for the simulations, up to a depth of 40 cm. Since the stoniness increases with depth below this level, the bulk density was kept at the 30–40 cm level below 40 cm. The bulk density for the L, F

and H horizons were set to typical values observed in the field. The bottom depth of the soil profile was set at 70 cm.

4. Results

4.1. Organic carbon stocks and mass fraction profile

Modeled organic carbon stocks and concentration profile for the reference simulation are shown together with measured values in figures 3 and 4 (center graphs). The modeled results are values from the last year of the spin-up, from a month near the sampling date, to reduce differences with measurements due to seasonal fluctuations.

The predicted stocks and concentrations generally compare well with measurements. However, the organic carbon stock in the F+H horizon is strongly overestimated with respect to the measurements. This may be caused by a too low bioturbation rate or too low decomposition rates of the organic carbon pools. The carbon stocks in the topsoil are underestimated while the subsoil stocks are overestimated. Presumably, a higher bioturbation rate and a lower advection rate would lead to a better fit to the measurements, but without additional data and more thorough calibration the precise reason cannot be determined. Furthermore, the possibility of a bias in the model results is higher for the deep soil, due to the presence of stones, which are not accounted for in SOMPROF.

Although leachable slow (LS) organic matter is absent in the organic layer, it is the largest organic matter pool (11.0 kgC m^{-2} of 15.4 kgC m^{-2} in total) due to its predicted abundance in the complete mineral soil profile. The importance of the LS pool is not surprising, given that it has the lowest decomposition rate of all pools. Fragmented litter dominates the upper 5 cm of the mineral soil, but decreases rapidly with depth, becoming negligible below 10 cm. The root litter and non-leachable slow (NLS) pool reach deeper levels because of direct local input and, in the case of NLS-OM, the relatively low decomposition rate.

4.2. Development of the organic carbon stocks

Figure 7 shows the development of the carbon pools for the reference simulation. Initially all material produced in the L horizon flows immediately into the mineral soil, preventing buildup of an F or H horizon. When the flux from the L layer exceeds the bioturbation rate, the F and H horizon start to form. In this case this occurs after approximately 50 years.

Under certain conditions, the organic carbon stock of the mineral soil initially increases, peaks, and then decreases again (figure 8). This is caused by a positive feedback in the formation of the F and H horizon due to the fact that root litter input of a layer is indirectly proportional to its mass (via its thickness, section 2.2). Initially, in absence of an F or H horizon, all root litter (and its decomposition products) flows into the mineral soil. As the organic layer develops, root litter input gradually shifts to the F and H horizon, leading to reduced organic matter input into the mineral soil.

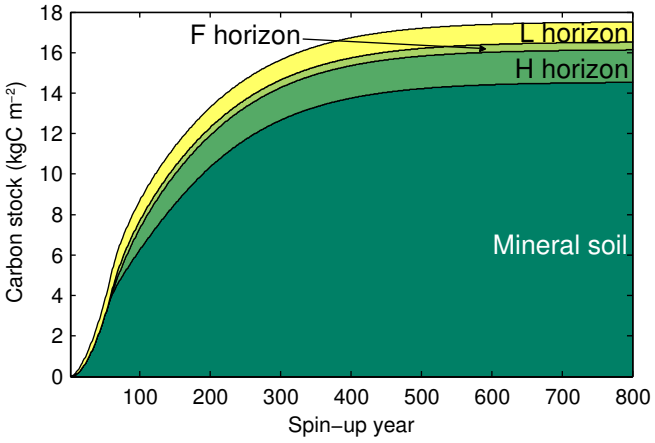

Figure 7: Development of the organic carbon stocks for for the reference simulation.

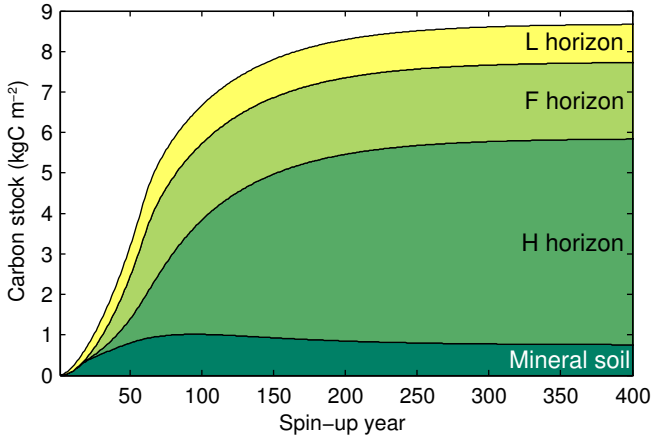

Figure 8: Development of the organic carbon stocks for a scenario with high and shallow root litter input and low bioturbation. Input parameters are as follows: $k_{NLS} = 0.02\,yr^{-1}$; $k_{LS} = 0.02\,yr^{-1}$; $\alpha_{AGL\to FL} = 0.7$; $\alpha_{FL\to NLS} = 0.1$; $\alpha_{FL\to LS} = 0.05$; $\alpha_{RL\to NLS} = 0.2$; $\alpha_{RL\to LS} = 0.05$; $B = 0.1\,kg\,m^{-2}\,yr^{-1}$; $\beta = 0.4\,m^{-1}$; $I_{RL} = 0.8\,kgC\,m^{-2}\,yr^{-1}$; all other parameters as listed in table 2.

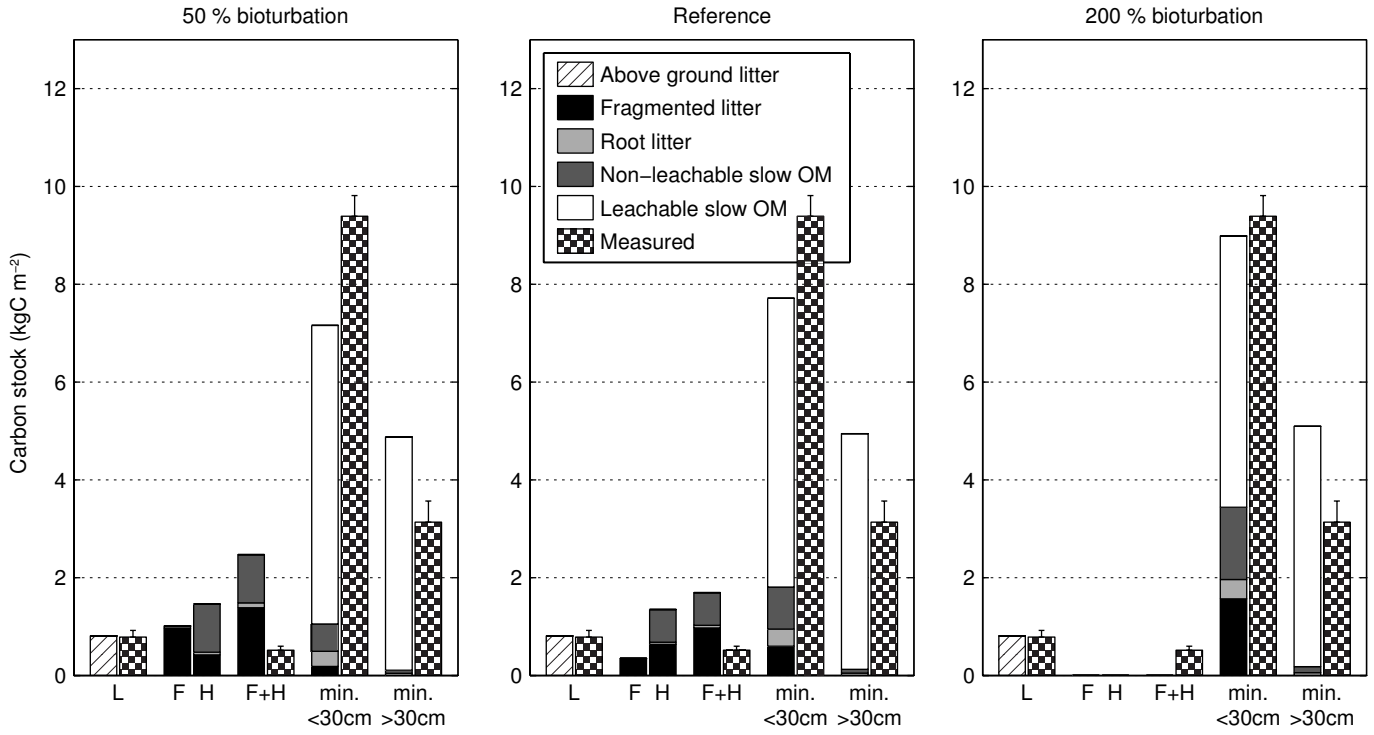

Figure 3: Measured organic carbon stocks and modeled stocks for three bioturbation scenarios: $B =$ 0.2, 0.4 and 0.8 kg m^{-2} yr^{-1}. All other parameters are as listed in table 2. Measured stocks are mean values; errorbars denote 1 standard error of the mean.

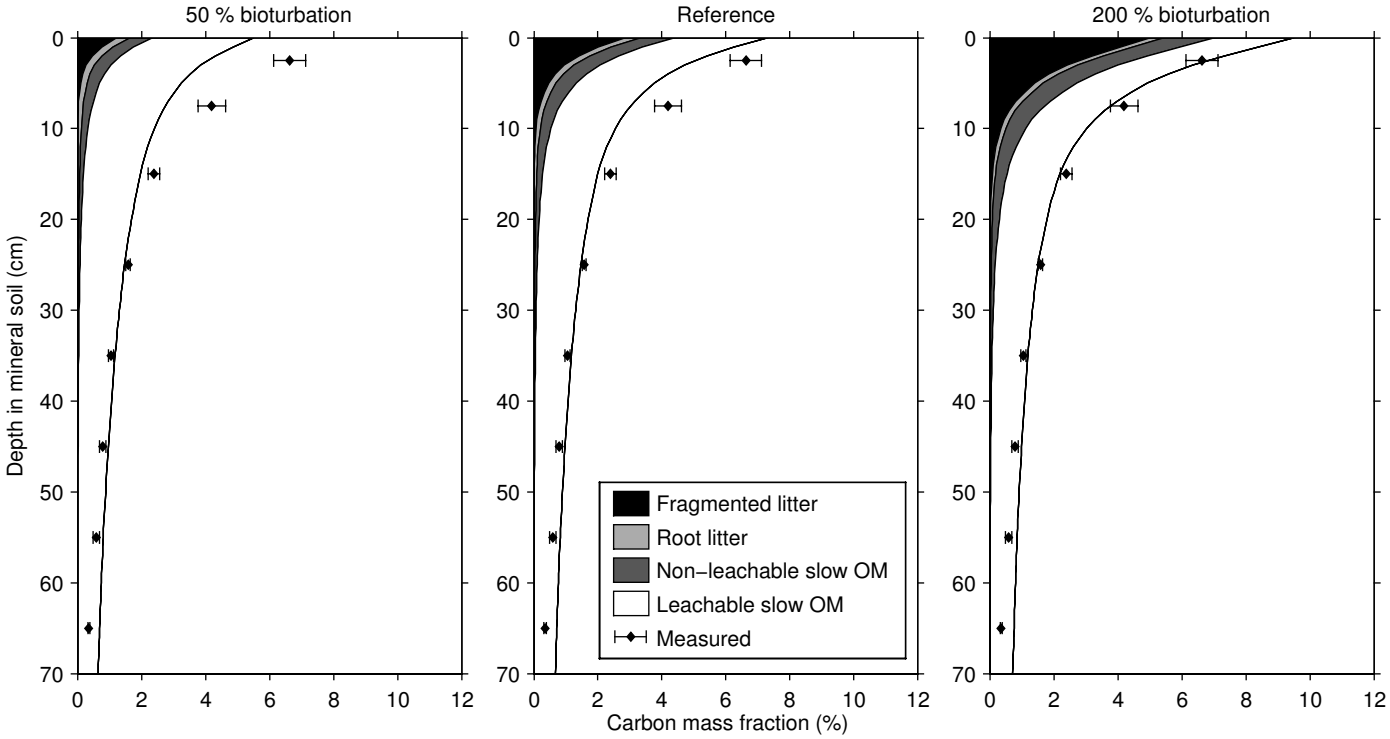

Figure 4: Measured organic carbon mass fraction profile in the mineral soil and modeled fraction profiles for three bioturbation scenarios: $B =$ 0.2, 0.4 and 0.8 kg m^{-2} yr^{-1}. All other parameters are as listed in table 2. Measured concentrations are mean values; errorbars denote 1 standard error of the mean.

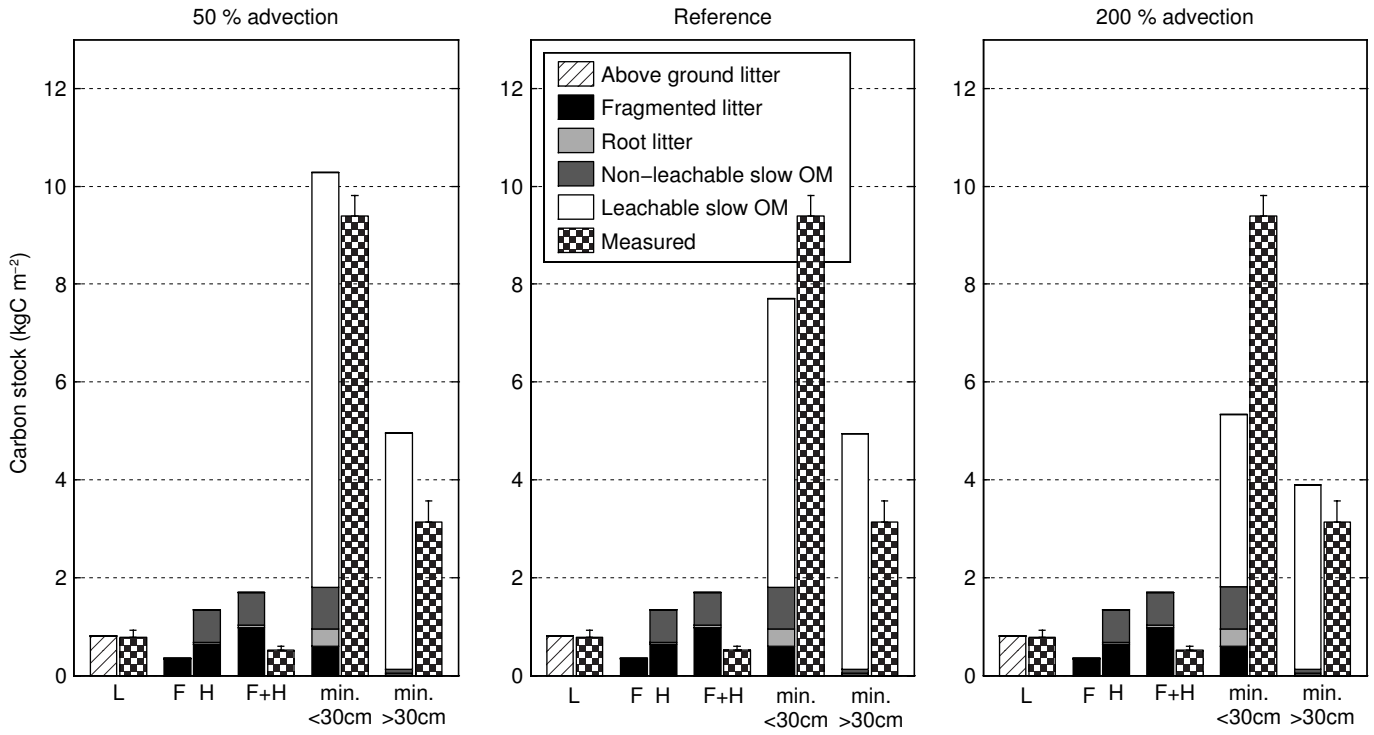

Figure 5: Measured organic carbon stocks and modeled stocks for three advection scenarios: $v =$ 0.001, 0.002 and 0.004 m yr^{-1}. All other parameters are as listed in table 2. Measured stocks are mean values; errorbars denote 1 standard error of the mean.

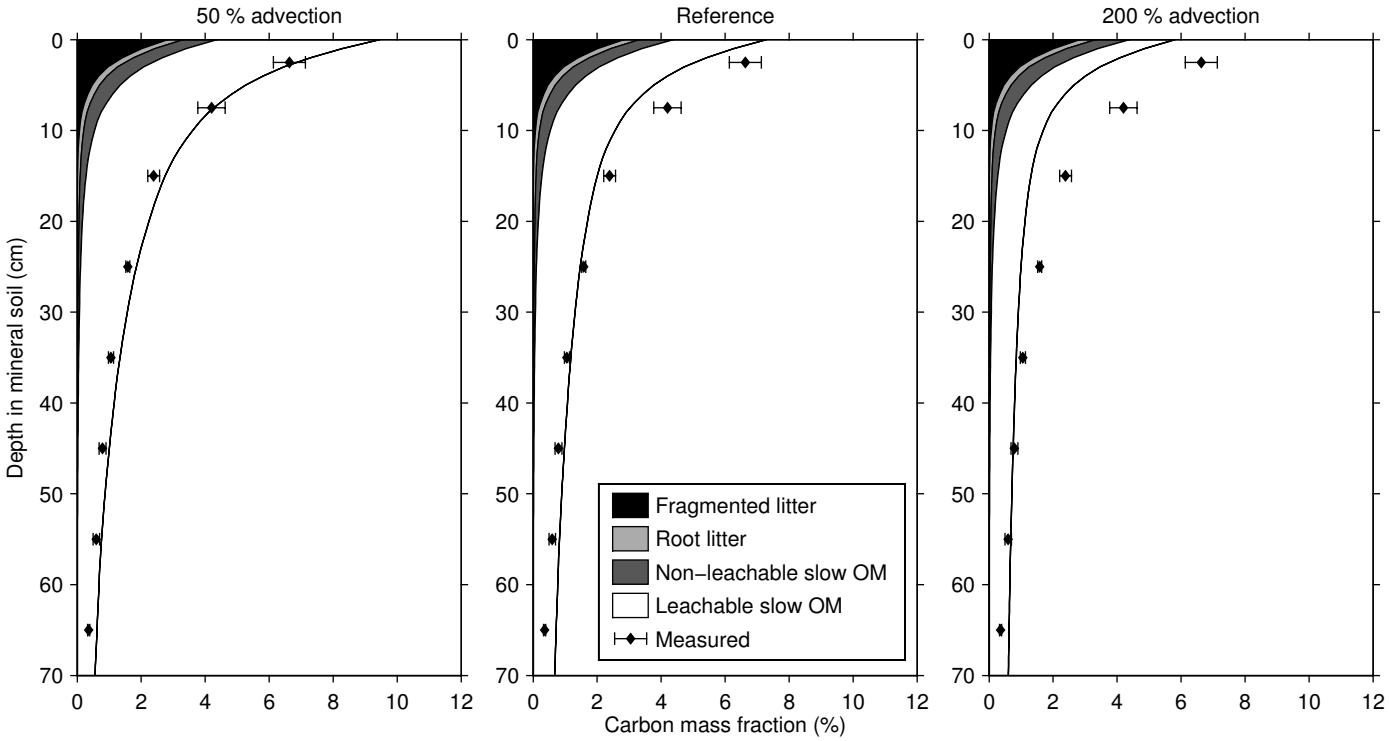

Figure 6: Measured organic carbon mass fraction profile in the mineral soil and modeled fraction profiles for three advection scenarios: $v =$ 0.001, 0.002 and 0.004 m yr^{-1}. All other parameters are as listed in table 2. Measured concentrations are mean values; errorbars denote 1 standard error of the mean.

4.3. Organic matter transport fluxes

Figure 9 depicts the different transport fluxes in the the mineral soil. The advective flux is clearly the main transport mechanism in virtually all of the soil profile. Only in the top 2 to 3 cm, is diffusion more important due to the high concentration gradient of fragmented litter there. The relative importance of advection for organic matter transport is caused mainly by the fact that leachable slow organic matter is the largest organic matter pool, due to its low decomposition rate. Interestingly, the diffusive transport rate of LS-OM near the surface is negative, indicating upward transport. This is because the LS-OM concentration peaks at around 5 cm depth, which indicates that the largest input of LS-OM due to root litter and fragmented litter decomposition is around this depth. Presumably, this is a modeling artifact and does not occur in reality.

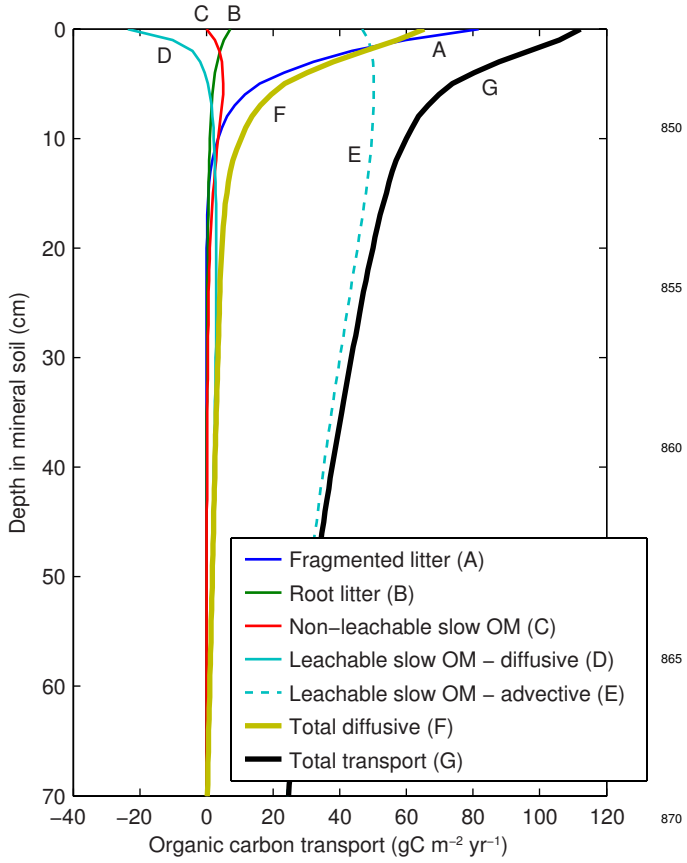

Figure 9: Organic carbon transport fluxes in the mineral soil for the reference simulation. Downward fluxes are positive.

4.4. Sensitivity to transport parameters

4.4.1. Bioturbation rate

The bioturbation rate B controls both the flow of organic matter from the organic horizons, as well as the diffusivity determining the transport within the mineral soil. The effects of a 50 % reduction and a 100 % increase of the bioturbation rate on the organic carbon stocks and organic carbon profile in the mineral soil are shown in figures 3 and 4, respectively. Increasing the bioturbation rate causes a shift of material from the organic layer to the mineral soil, leading to complete disappearance of the F and H horizon in the high bioturbation scenario.

The effects of bioturbation are mostly limited to the fragmented litter and non-leachable slow pools. These pools are dependent on bioturbation for downward flow, whereas root litter and leachable slow organic matter are also influenced by direct input and advection, respectively. The change of bioturbation rate has virtually no influence on the carbon stocks below 50 cm.

4.4.2. Advection rate

Figures 5 and 6 show the organic carbon stocks for the control, a 50 % decrease and a 100 % increase of the advection rate. As would be expected, the advection rate has no influence on the stocks in the organic layers since it does not affect the flow into the mineral soil. The mineral soil stock of leachable slow organic matter strongly decreases with increasing advection rate, particularly in the the topsoil. This is explained by the increased loss of organic carbon over the lower boundary. Interestingly, the organic matter concentration below 50 cm is slightly lower both for the scenario with increased advection and with decreased advection, with respect to the reference simulation. The reason for this is that for the low advection scenario less LS-OM reaches the subsoil, while for the high advection scenario more LS-OM flows out of the system over the lower boundary, both cases leading to lower organic matter concentrations.

The amount of carbon lost at the lower boundary is also strongly dependent on the advection rate: 9.36 gC m^{-2} yr^{-1} for the low advection scenario, 22.6 gC m^{-2} yr^{-1} for the reference and 34.7 gC m^{-2} yr^{-1} for the high advection scenario.

4.5. Influence of the SOM profile on heterotrophic respiration

To study the effects of the vertical SOM distribution on heterotrophic respiration, we set up three SOMPROF simulations with different vertical organic matter distributions, by varying the transport rates and the vertical distribution of root litter input (figure 10). The lower boundary of the mineral soil was set to 3 m to assure that virtually all SOM is accounted for in the simulations, and differences in predicted respiration are not due to differences in total carbon stock. Since soil moisture measurements were available only up to a depth of 32 cm, the soil moisture is estimated by non-linear extrapolation up to a depth of 70 cm. Below 70 cm, the soil moisture was held at a constant value.

Figure 11 shows the relative contribution of the three organic horizons and the mineral soil to the total heterotrophic respiration, for the three scenarios. The vertical organic matter distribution strongly influences the location of the CO_2 production within the profile. Aside from short time scale fluctuations, this vertical partitioning is quite constant, showing little seasonal variability. A notable exception is the summer of 2003, which was an exceptionally dry and hot period in Europe. During this time, soil moisture decreased severely at Hainich, with lowest values in the organic layer and in the topsoil (figure 2). The

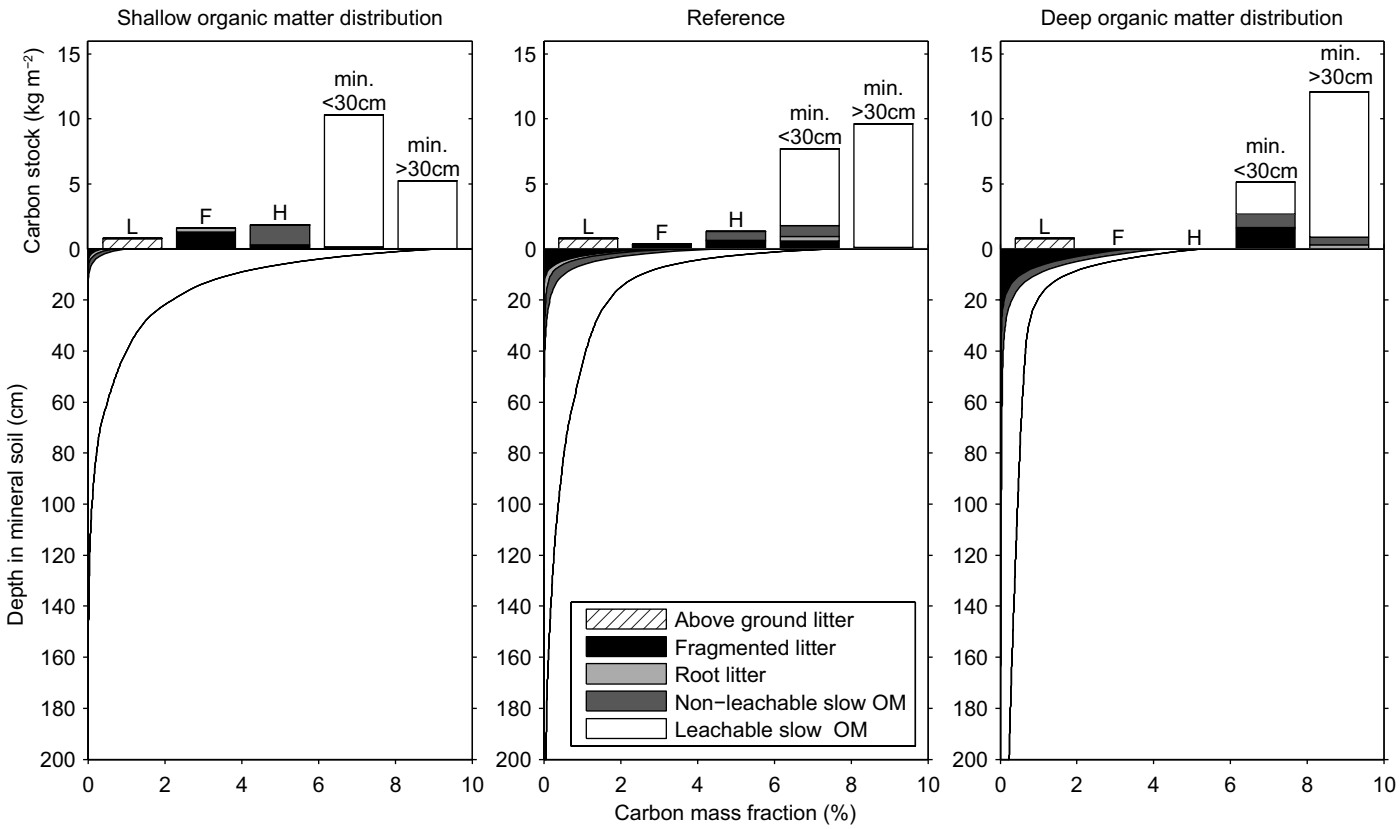

Figure 10: Carbon stocks and profile for of the three scenarios used to study the effects of the organic matter distribution on heterotrophic respiration. Parameters are as follows: Shallow organic matter distribution: $\beta = 0.4\,\mathrm{m}^{-1}$; $B = 0.25\,\mathrm{kg\,m^{-2}\,yr^{-1}}$ $v = 0.001\,\mathrm{m\,yr^{-1}}$. Deep organic matter distribution: $\beta = 0.01\,\mathrm{m}^{-1}$; $B = 2\,\mathrm{kg\,m^{-2}\,yr^{-1}}$ $v = 0.002\,\mathrm{m\,yr^{-1}}$. For all three scenarios the depth of the lower boundary has been set to 3 m. All other parameters, as well as all parameters for the reference scenario are as listed in table 2.

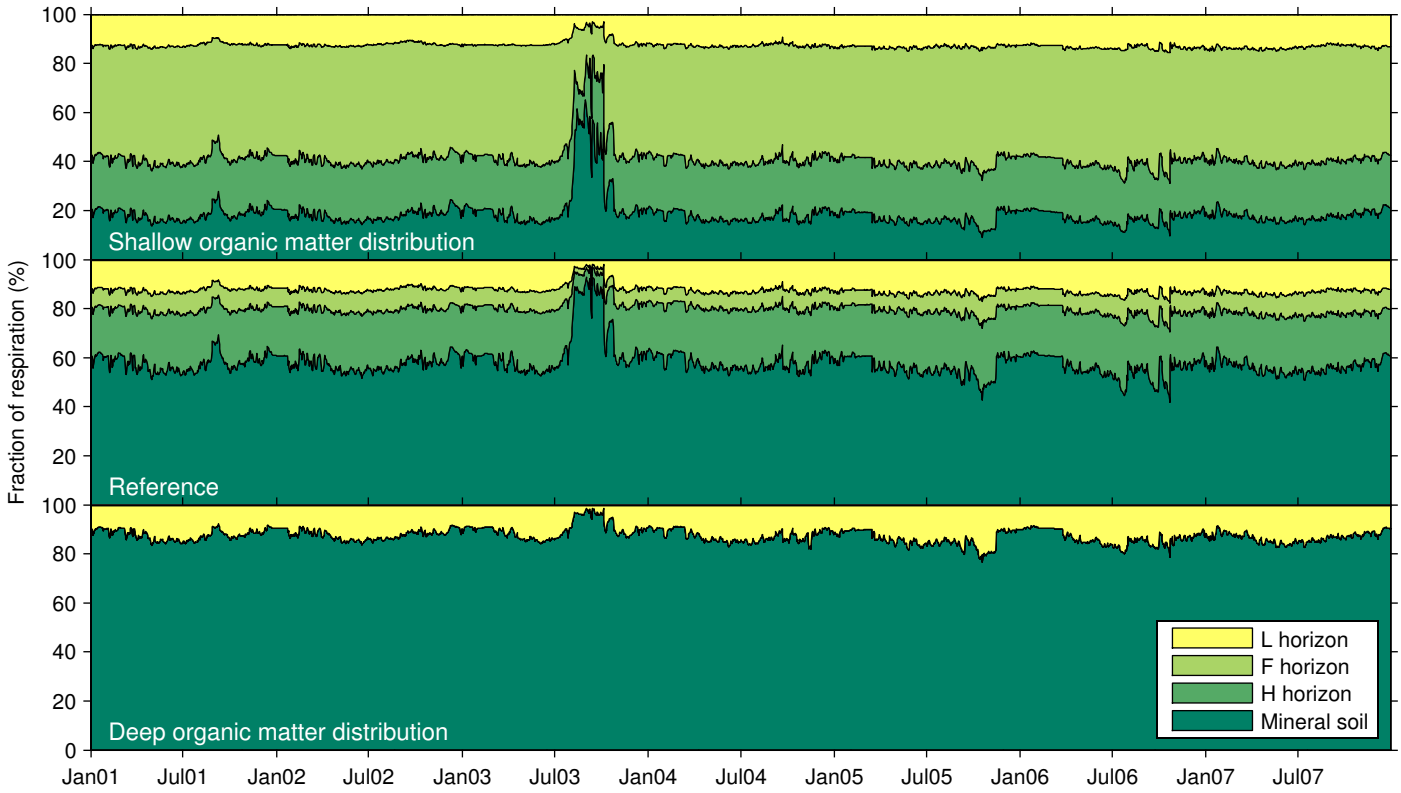

Figure 11: Relative contribution of the three organic horizons and the mineral soil of the three organic matter distribution scenarios for the simulation period.

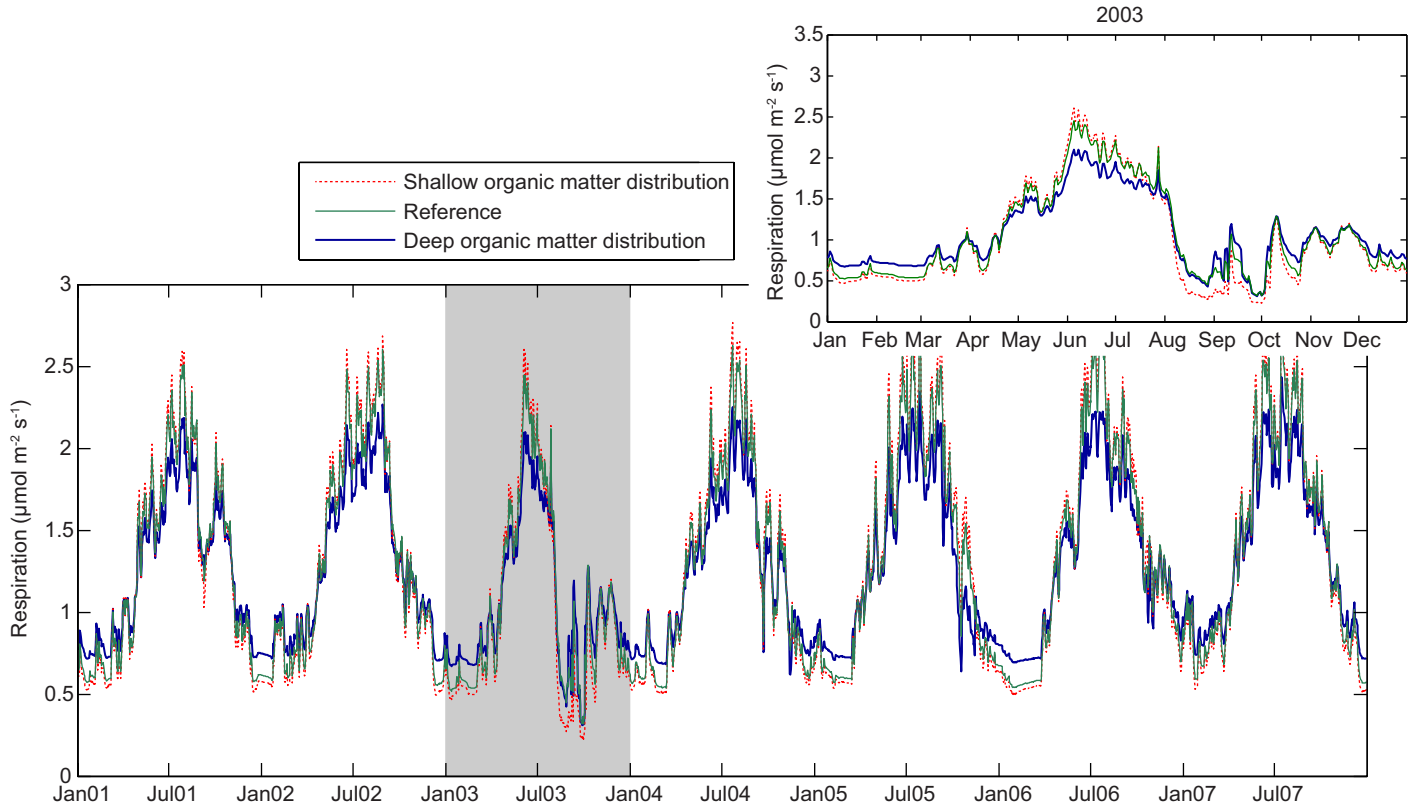

Figure 12: Total heterotrophic respiration of the three organic matter distribution scenarios for the simulation period.

vertical partitioning of the heterotrophic respiration changes dramatically during the drought: the mineral soil becomes the dominating source of CO_2 in all three scenarios. These marked differences demonstrate the severity of the drought.

The vertical organic matter distribution also has a significant effect on the temporal variation of total heterotrophic respiration, as shown in figure 12. The amplitude of the fluctuations decreases with deeper organic matter distribution: the deep organic matter scenario has lower respiration rates in summer and higher rates in winter, compared to the other scenarios. Also the response to the 2003 drought (figure 12, inset) is less pronounced for the deep organic matter scenario, although the differences are relatively small because ultimately the whole profile was affected by the drought.

5. Discussion

5.1. Organic carbon stocks and profile

The results depicted in figures 3-6 show that SOMPROF is able to produce organic carbon stocks and profiles that are realistic compared to measurements. Furthermore, it does so based on input parameter values that lie within ranges suggested by *a priori* knowledge (section 2.7), which is encouraging. It must be noted, however, that the model is over-parameterized with respect to the available measurements. This is clear, for example, from the fact that the profile and stocks are roughly equally well reproduced in the high bioturbation scenario (figures 3 and 4, right graphs) and the low advection scenario (figures 5 and 6 left graphs), which have distinctly different parameter sets.

In spite of this problem, the results offer some insight into the structure of the mineral SOM profile (figures 4 and 6). The profile can be divided into a zone near the surface with relatively fast decay of organic matter content with depth, and a zone with a smaller depth gradient in the subsoil. The model results suggest that the two zones are characterized by different organic matter deposition mechanisms: bioturbation in the topsoil and liquid phase transport in the subsoil. The low depth gradient in the subsoil causes a long, downward "tail" of organic matter, which is also often observed in the field. Because of this tail, a power function of depth often yields a better fit to the vertical SOM profile than a one-term exponential decay function (Jobbagy and Jackson, 2000).

In the model results, the leachable slow organic matter pool is dominant throughout most of the profile. This can fully be ascribed to our choice for model parameters: its decomposition rate is lowest of all pools, while it is formed at the same rate as non-leachable slow OM. Nevertheless, measurements at Hainich (Schrumpf, unpublished) show that most organic matter is located in the heavy fraction. Since the heavy fraction can be assumed to be mineral associated organic matter, this corroborates our results.

The positive feedback in the development of the F and H horizon (section 4.2) leads, under certain conditions, to interesting behavior in which the mineral soil carbon stock initially increases and later decreases again (figure 8). Although the F/H horizon feedback always occurs if these layers are present, the peaking behavior of the mineral soil stock is observed only in situations where root litter input is the dominant source of organic matter, while being shallowly distributed in the profile. Furthermore, vertical transport of organic matter should play a small role, which means that the mineral soil is mostly dependent on root litter for its soil carbon input. Such conditions may occur, for example, in a forest on a poor soil (i.e. with little soil biological activity) with a productive herbaceous understorey. Although it does not seem unlikely that the predicted behavior could occur for such a site, we did not find chronosequence studies that confirm this, since soil carbon buildup usually involves a succession of vegetation types, accompanied by changes in (root) litter production.

5.2. Soil organic matter transport

In our simulations, liquid phase transport of organic matter is the dominant mechanism for SOM movement in most of the profile, due to the abundance of LS-OM (figure 9). Thorough parameter estimation should reveal if this is truly the case for Hainich. However, even if advection dominates, bioturbation should not be ignored as mechanism for organic matter transport. The bioturbation rate strongly controls the organic carbon stocks in the F and H horizons and determines the amount of easily decomposable material in the topsoil.

SOMPROF behaves differently with respect to bioturbation than existing models that include this process: for a small increase of bioturbation, the increased input of organic matter into the mineral soil is not fully compensated by the increased diffusion rate, leading to *higher* concentrations in the topsoil. Only in absence of an F and H horizon, will an increase of bioturbation rate lead to reduced organic matter concentrations due to faster diffusion. In this respect SOMPROF is more realistic than SOM profile models that ignore the organic layer. This is corroborated by results of Alban and Berry (1994) who found a significant increase of topsoil organic carbon content together with a decrease of organic layer mass for a forest soil which was invaded by earthworms.

Predicted organic carbon loss over the lower boundary due to advection (section 4.4.2) is strongly overestimated compared to *in situ* measurements at Hainich by Kindler et al. (2010), who found fluxes of 1.9–2.6 $\mathrm{gC\,m^{-2}\,yr^{-1}}$ from the subsoil. The advective loss rates are also relatively high compared to typically observed estimates at other sites (Michalzik et al., 2001). This points to a too high advection rate in the deep soil, which may also partly explain the overestimation of the deep soil organic matter concentration. It is likely that the advection rate of the deep soil is in reality lower than that of the topsoil, since average water infiltration rates decrease with depth (Sanderman et al., 2008). At Hainich this is particularly likely due to the high clay content which obstructs water drainage and adsorbs organic matter. The predicted advective loss of organic matter also depends on the depth at which the lower boundary is set in the model. Leached organic matter can be accounted for simply by lowering the soil depth (compare figures 3 and 4 with figure 10, middle graphs). This raises the question whether leached organic carbon in the field can really be considered lost or if it

is retained by adsorption at depths below the lowest measurement depth, in which case it may still contribute to respiration.

5.3. Significance of the SOM profile for carbon cycling

The results in section 4.5 demonstrate that the vertical SOM distribution can significantly affect soil carbon cycling at short time scales. Since temporal fluctuations of soil moisture and temperature decrease with depth in soil, a deeper distribution of organic matter causes reduced variability of heterotrophic respiration. This suggests that a soil with a deep SOM distribution is less sensitive to short timescale climatic fluctuations than a soil with a shallow distribution. However, since no measurements of soil moisture and temperature were available below 32 and 50 cm respectively, we needed to make assumptions regarding these quantities in the deep soil. A more thorough modelling study is needed to evaluate these effects.

Whether these interactions affect the average long term soil carbon balance is unsure, since, in this case, the vertical SOM distribution affects mostly the amplitude and less the average of the variations. In general, the long term effects depend on the non-linearity of the of the response functions and the average vertical gradients of the temperature moisture profiles. This suggests that the variability of soil moisture would play a greater role on the long time scale, since its response function is less linear and it generally displays stronger depth gradients than soil temperature. More simulation studies, for different conditions and at larger spatial scales (possibly as part of a dynamic global vegetation model) should reveal if these effects truly play a significant role for soil carbon cycling.

A large part of the merit of a vertically explicit SOM model lies in synergies with other processes that are not yet implemented in SOMPROF. For example, the vertical SOM profile (particularly the presence of an organic surface layer) strongly influences soil heat and moisture transport (Koven et al., 2009; Lawrence and Slater, 2008), which ultimately feed back to soil carbon cycling. Also microbial dynamics may be of importance on long time scales (Fontaine et al., 2007; Allison et al., 2010). Fontaine et al. (2007) showed that deep soil organic carbon can be stabilized due to the absence of fresh organic matter for microbial decomposers. A decomposition model that includes such effects, as part of a vertically explicit scheme, is likely to find markedly different results for deep soil carbon storage.

5.4. Model limitations

SOMPROF cannot be applied under all conditions. The organic layer structure corresponds to the humus profile observed in forests. For grassland soils it may not be possible to make the distinction between an organic layer and the mineral soil, since organic matter accumulation occurs mostly in the topsoil due to root turnover. Furthermore, SOMPROF is not suitable for soils where the vertical SOM profile is significantly influenced by processes that are not represented, including ploughing, cryoturbation, erosion and podzolization.

Currently, SOMPROF does not account for stones in the mineral soil matrix. To include these effects the mass balance equations would need to be corrected for the amount of fine soil that is involved with carbon storage and bioturbation. Since the high stone content at Hainich is limited to the deep soil where organic carbon fractions are low, presumably the error in the predicted carbon stocks are small. However, many soils have a high stoniness throughout the profile, which significantly affects the vertical SOM distribution.

Future model development will address several of the issues discussed above to improve the large scale applicability of the model.

5.5. Outlook

For further application of SOMPROF, parameter estimation is required to obtain insight into the model parameters, particularly those related to SOM transport, since they are relatively unknown. A problem is posed by equifinality: the ability of the model to produce similar results using significantly different parameter sets. The fact that the different mathematical terms in SOMPROF relate to specific processes somewhat alleviates this problem because it allows *a priori* rough estimates of parameter values to be obtained. Nevertheless, future model testing should investigate whether the model may be simplified in order to facilitate parameter estimation. Furthermore, observational data used for optimization should include additional high-resolution profile data, such as ^{14}C and ^{13}C measurements and respiration rates. Also, since small scale spatial heterogeneity can significantly affect local stocks and profiles, multiple replicate samplings at different locations within one ecosystem or soil type are required.

Application of the model at large spatial scales requires sets of parameters for different ecosystems and soils, or empirical functions relating the parameters to information in available data sets. Bioturbation is strongly linked to climate, litter quality and soil properties such as pH and base saturation. Since conditions that support a high vegetation productivity and litter quality tend to have a large and active soil fauna community as well, vegetation type and productivity may be a good proxy for the bioturbation rate. The advection rate is related to physical and chemical factors, such as water infiltration rates, soil texture, and pH.

It is likely that the spatial variability of the transport parameters is comparable to that of the decomposition parameters since both groups are influenced by the same environmental factors. Therefore, we do not expect that the introduction of a vertical scheme in SOM models as such calls for better representation of spatial heterogeneity compared to current models.

Many existing SOM models can be made vertically explicit by adopting the scheme of SOMPROF. This modification would mainly involve separation of the soil into the mineral soil with a concentration profile, and the organic layer, possibly further subdivided into different horizons. The pool structure of the model to be adjusted must support the change of transport behavior during the decomposition process. Hence, a serial arrangement of pools (with one type of material being transformed to another) is preferable. Furthermore, a specific pool must be defined that is transported advectively, to represent liquid phase mediated transport. Finally, there must be an explicit

distinction between above ground litter and root litter, since these two types represent different input mechanisms.

6. Conclusions

SOMPROF is able to reproduce organic carbon stocks and concentration profiles that compare well to measurements, using input parameters that are reasonable compared to prior knowledge. Furthermore, the model is able to produce widely different organic matter profiles, making it applicable to a range of soil types, provided that the natural process of soil formation has not been disturbed. The model can provide insight into several processes that cannot be addressed with bulk models, such as soil formation, organic matter origin, loss of organic carbon through leaching, and interactions between the SOM profile, heterotrophic respiration and soil temperature and moisture.

Acknowledgements

We thank Werner Kutsch for providing above ground and root litter production data for Hainich, and Olaf Kolle for providing soil temperature and moisture measurements. We are grateful to Bas Kempen and two anonymous reviewers for helpful comments on the manuscript draft. This work was supported by the ERC starting grant QUASOM (ERC-2007-StG-208516).

References

Alban, D.H., Berry, E.C., 1994. Effects of earthworm invasion on morphology, carbon, and nitrogen of a forest soil. Applied Soil Ecology 1, 243–249.

Allison, S.D., Wallenstein, M.D., Bradford, M.A., 2010. Soil-carbon response to warming dependent on microbial physiology. Nature Geoscience 3, 336–340.

Baisden, W.T., Amundson, R., Brenner, D.L., Cook, A.C., Kendall, C., Harden, J.W., 2002. A multiisotope C and N modeling analysis of soil organic matter turnover and transport as a function of soil depth in a california annual grassland soil chronosequence. Global Biogeochemical Cycles 16, 82.

Batjes, N.H., 1996. Total carbon and nitrogen in the soils of the world. European Journal of Soil Science 47, 151–163.

Berg, B., McClaugherty, C., 2003. Plant litter: decomposition, humus formation, carbon sequestration. Springer, Berlin [u.a.]. second edition.

Bosatta, E., Ågren, G.I., 1996. Theoretical analyses of carbon and nutrient dynamics in soil profiles. Soil Biology and Biochemistry 28, 1523–1531.

Boudreau, B.P., 1986. Mathematics of tracer mixing in sediments; i, spatially-dependent, diffusive mixing. American Journal of Science 286, 161–198.

Bruun, S., Christensen, B.T., Thomsen, I.K., Jensen, E.S., Jensen, L.S., 2007. Modeling vertical movement of organic matter in a soil incubated for 41 years with ^{14}C labeled straw. Soil Biology and Biochemistry 39, 368–371.

Cesarz, S., Fahrenholz, N., Migge-Kleian, S., Platner, C., Schaefer, M., 2007. Earthworm communities in relation to tree diversity in a deciduous forest. European Journal of Soil Biology 43, S61–S67.

Conant, R.T., Steinweg, J.M., Haddix, M.L., Paul, E.A., Plante, A.F., Six, J., 2008. Experimental warming shows that decomposition temperature sensitivity increases with soil organic matter recalcitrance. Ecology 89, 2384–2391.

van Dam, D., Veldkamp, E., van Breemen, N., 1997. Soil organic carbon dynamics: variability with depth in forested and deforested soils under pasture in Costa Rica. Biogeochemistry 39, 343–375.

Davidson, E.A., Janssens, I.A., 2006. Temperature sensitivity of soil carbon decomposition and feedbacks to climate change. Nature 440, 165–173.

Davidson, E.A., Savage, K.E., Trumbore, S.E., Borken, W., 2006. Vertical partitioning of CO_2 production within a temperate forest soil. Global Change Biology 12, 944–956.

van Delft, B., de Waal, R., Kemmers, R., Mekkink, P., Sevink, J., 2006. Field guide humus forms, description and classification of humus forms for ecological applications. Technical Report. Alterra, Research Institute for the Green Environment. http://www.humusvormen.wur.nl/UK/.

Diochon, A.C., Kellman, L., 2009. Physical fractionation of soil organic matter: Destabilization of deep soil carbon following harvesting of a temperate coniferous forest. Journal of Geophysical Research-Biogeosciences 114, G01016.

Dörr, H., Münnich, K.O., 1989. Downward movement of soil organic matter and its influence on trace-element transport (^{210}Pb, ^{137}Cs) in the soil. Radiocarbon 31, 655–663.

Drigo, B., Kowalchuk, G.A., van Veen, J.A., 2008. Climate change goes underground: effects of elevated atmospheric CO_2 on microbial community structure and activities in the rhizosphere. Biology and Fertility of Soils 44, 667–679.

Elzein, A., Balesdent, J., 1995. Mechanistic simulation of vertical distribution of carbon concentrations and residence times in soils. Soil Science Society of America Journal 59, 1328–1335.

Fang, C.M., Smith, P., Moncrieff, J.B., Smith, J.U., 2005. Similar response of labile and resistant soil organic matter pools to changes in temperature. Nature 433, 57–59.

Federer, C.A., Turcotte, D.E., Smith, C.T., 1993. The organic fraction bulk density relationship and the expression of nutrient content in forest soils. Canadian Journal of Forest Research-Revue Canadienne De Recherche Forestiere 23, 1026–1032.

Fierer, N., Chadwick, O.A., Trumbore, S.E., 2005. Production of CO_2 in soil profiles of a California annual grassland. Ecosystems 8, 412–429.

Fontaine, S., Barot, S., Barre, P., Bdioui, N., Mary, B., Rumpel, C., 2007. Stability of organic carbon in deep soil layers controlled by fresh carbon supply. Nature 450, 277–U10.

Freier, K.P., Glaser, B., Zech, W., 2010. Mathematical modeling of soil carbon turnover in natural podocarpus forest and eucalyptus plantation in Ethiopia using compound specific delta 13c analysis. Global Change Biology 16, 1487–1502.

Friedlingstein, P., Cox, P., Betts, R., Bopp, L., Von Bloh, W., Brovkin, V., Cadule, P., Doney, S., Eby, M., Fung, I., Bala, G., John, J., Jones, C., Joos, F., Kato, T., Kawamiya, M., Knorr, W., Lindsay, K., Matthews, H.D., Raddatz, T., Rayner, P., Reick, C., Roeckner, E., Schnitzler, K.G., Schnur, R., Strassmann, K., Weaver, A.J., Yoshikawa, C., Zeng, N., 2006. Climate-carbon cycle feedback analysis: Results from the C^4MIP model intercomparison. Journal of Climate 19, 3337–3353.

Gregorich, E.G., Ellert, B.H., Drury, C.F., Liang, B.C., 1996. Fertilization effects on soil organic matter turnover and corn residue C storage. Soil Science Society of America Journal 60, 472–476.

Hashimoto, S., Tanaka, N., Kume, T., Yoshifuji, N., Hotta, N., Tanaka, K., Suzuki, M., 2007. Seasonality of vertically partitioned soil CO_2 production in temperate and tropical forest. Journal of Forest Research 12, 209–221.

Heimann, M., Reichstein, M., 2008. Terrestrial ecosystem carbon dynamics and climate feedbacks. Nature 451, 289–292.

Hinze, J., 1975. Turbulence. McGraw-Hill series in mechanical engineering, McGraw-Hill, New York. second edition.

Hoosbeek, M.R., Scarascia-Mugnozza, G.E., 2009. Increased litter build up and soil organic matter stabilization in a poplar plantation after 6 years of atmospheric CO_2 enrichment (FACE): Final results of POP-EuroFACE compared to other forest FACE experiments. Ecosystems 12, 220–239.

Huang, K., Toride, N., Genuchten, M.T., 1995. Experimental investigation of solute transport in large, homogeneous and heterogeneous, saturated soil columns. Transport in Porous Media 18, 283–302.

IUSS Working Group WRB, 2007. World Reference Base for Soil Resources 2006, first update 2007. Technical Report. FAO.

Iversen, C.M., 2010. Digging deeper: fine-root responses to rising atmospheric CO_2 concentration in forested ecosystems. New Phytologist 186, 346–357.

Jardine, P.M., Wilson, G.V., Luxmoore, R.J., McCarthy, J.F., 1989. Transport of inorganic and natural organic tracers through an isolated pedon in a forest watershed. Soil Science Society of America Journal 53, 317–323.

Jenkinson, D.S., 1990. The turnover of organic carbon and nitrogent in soil. Philosophical Transactions of the Royal Society of London Series B-Biological Sciences 329, 361–368.

Jenkinson, D.S., Coleman, K., 2008. The turnover of organic carbon in subsoils. part 2. modelling carbon turnover. European Journal of Soil Science 59, 400–413.

Jenkinson, D.S., Rayner, J.H., 1977. Turnover of soil organic matt in some of the Rothamsted classical experiments. Soil Science 123, 298–305.

Jobbagy, E.G., Jackson, R.B., 2000. The vertical distribution of soil organic carbon and its relation to climate and vegetation. Ecological Applications 10, 423–436.

Jones, C., McConnell, C., Coleman, K., Cox, P., Falloon, P., Jenkinson, D., Powlson, D., 2005. Global climate change and soil carbon stocks; predictions from two contrasting models for the turnover of organic carbon in soil. Global Change Biology 11, 154–166.

Jones, C.D., Cox, P., Huntingford, C., 2003. Uncertainty in climate-carbon-cycle projections associated with the sensitivity of soil respiration to temperature. Tellus Series B-Chemical and Physical Meteorology 55, 642–648.

Kaiser, K., Guggenberger, G., 2000. The role of DOM sorption to mineral surfaces in the preservation of organic matter in soils. Organic Geochemistry 31, 711–725.

Kalbitz, K., Kaiser, K., 2008. Contribution of dissolved organic matter to carbon storage in forest mineral soils. Journal of Plant Nutrition and Soil Science 171, 52–60.

Kalbitz, K., Solinger, S., Park, J.H., Michalzik, B., Matzner, E., 2000. Controls on the dynamics of dissolved organic matter in soils: A review. Soil Science 165, 277–304.

Kaste, J.M., Heimsath, A.M., Bostick, B.C., 2007. Short-term soil mixing quantified with fallout radionuclides. Geology 35, 243–246.

Kindler, R., Siemens, J., Kaiser, K., Walmsley, D., Bernhofer, C., Buchmann, N., Cellier, C., Eugster, W., Gleixner, G., Grünwald, T., Heim, A., Ibrom, A., Jones, S., Jones, M., Klumpp, K., Kutsch, W., Steenberg Larsen, K., Simon Lehuger, S., Loubet, B., McKenzie, R., Moors, E., Osborne, B., Pilegaard, K., Rebmann, C., Saunders, M., Schmidt, M.W., Schrumpf, M., Seyfferth, J., Skiba, U., Soussana, J., Sutton, M., Tefs, C., Vowinckel, B., Zeeman, M., Kaupenjohan, M., 2010. Dissolved carbon leaching from soil is a crucial component of the net ecosystem carbon balance. Accepted for publication in Global Change Biology.

Knorr, W., Prentice, I.C., House, J.I., Holland, E.A., 2005. Long-term sensitivity of soil carbon turnover to warming. Nature 433, 298–301.

Koven, C., Friedlingstein, P., Ciais, P., Khvorostyanov, D., Krinner, G., Tarnocai, C., 2009. On the formation of high-latitude soil carbon stocks: Effects of cryoturbation and insulation by organic matter in a land surface model. Geophysical Research Letters 36, L21501.

Kutsch, W., Persson, T., Schrumpf, M., Moyano, F., Mund, M., Andersson, S., Schulze, E.D., 2010. Heterotrophic soil respiration and soil carbon dynamics in the deciduous Hainich forest obtained by three approaches. Biogeochemistry -, 1–17.

Lawrence, D.M., Slater, A.G., 2008. Incorporating organic soil into a global climate model. Climate Dynamics 30, 145–160.

Lebret, M., Nys, C., Forgeard, F., 2001. Litter production in an Atlantic beech (*Fagus sylvatica* L.) time sequence. Annals of Forest Science 58, 755–768.

Lloyd, J., Taylor, J.A., 1994. On the temperature dependence of soil respiration. Functional Ecology 8, 315–323.

Lorenz, K., Lal, R., 2005. The depth distribution of soil organic carbon in relation to land use and management and the potential of carbon sequestration in subsoil horizons, in: Advances in Agronomy, Vol 88. Elsevier Academic Press Inc, San Diego. volume 88 of *Advances in Agronomy*, pp. 35–66.

von Lützow, M., Kögel-Knabne, I., Ludwig, B., Matzner, E., Flessa, H., Ekschmitt, K., Guggenberger, G., Marschner, B., Kalbitz, K., 2008. Stabilization mechanisms of organic matter in four temperate soils: Development and application of a conceptual model. Journal of Plant Nutrition and Soil Science 171, 111–124.

von Lützow, M., Kögel-Knabner, I., Ekschmitt, K., Matzner, E., Guggenberger, G., Marschner, B., Flessa, H., 2006. Stabilization of organic matter in temperate soils: mechanisms and their relevance under different soil conditions - a review. European Journal of Soil Science 57, 426–445.

Manzoni, S., Porporato, A., 2009. Soil carbon and nitrogen mineralization: Theory and models across scales. Soil Biology & Biochemistry 41, 1355–1379.

Meysman, F.J.R., Boudreau, B.P., Middelburg, J.J., 2003. Relations between local, nonlocal, discrete and continuous models of bioturbation. Journal of Marine Research 61, 391–410.

Meysman, F.J.R., Middelburg, J.J., Heip, C.H.R., 2006. Bioturbation: a fresh look at Darwin's last idea. Trends in Ecology and Evolution 21, 688–695.

Michalzik, B., Kalbitz, K., Park, J.H., Solinger, S., Matzner, E., 2001. Fluxes and concentrations of dissolved organic carbon and nitrogen - a synthesis for temperate forests. Biogeochemistry 52, 173–205.

Michalzik, B., Tipping, E., Mulder, J., Lancho, J.F.G., Matzner, E., Bryant, C.L., Clarke, N., Lofts, S., Esteban, M.A.V., 2003. Modelling the production and transport of dissolved organic carbon in forest soils. Biogeochemistry 66, 241–264.

Nakane, K., Shinozaki, K., 1978. A mathematical model of the behavior and vertical distribution of organic carbon in forest soils. Japanese Journal of Ecology 28, 111–122.

Neff, J.C., Asner, G.P., 2001. Dissolved organic carbon in terrestrial ecosystems: Synthesis and a model. Ecosystems 4, 29–48.

Nodvin, S.C., Driscoll, C.T., Likens, G.E., 1986. Simple partitioning of anions and dissolved organic carbon in a forest soil. Soil Science 142, 27–35.

Norby, R.J., DeLucia, E.H., Gielen, B., Calfapietra, C., Giardina, C.P., King, J.S., Ledford, J., McCarthy, H.R., Moore, D.J.P., Ceulemans, R., De Angelis, P., Finzi, A.C., Karnosky, D.F., Kubiske, M.E., Lukac, M., Pregitzer, K.S., Scarascia-Mugnozza, G.E., Schlesinger, W.H., Oren, R., 2005. Forest response to elevated CO_2 is conserved across a broad range of productivity. Proceedings of the National Academy of Sciences of the United States of America 102, 18052–18056.

O'Brien, B.J., Stout, J.D., 1978. Movement and turnover of soil organic matter as indicated by carbon isotope measurements. Soil Biology and Biochemistry 10, 309–317.

Parton, W.J., Schimel, D.S., Cole, C.V., Ojima, D.S., 1987. Analysis of factors controlling soil organic matter levels in Great Plains grasslands. Soil Science Society of America Journal 51, 1173–1179.

Paton, T., Humphreys, G.S., Mitchell, P., 1995. Soils: a new global view. Yale Univ. Press, New Haven [u.a.]. chapter 3. Bioturbation. pp. 33–67.

Paustian, K., Ågren, G., Bosatta, E., 1997. Modeling litter quality effects on decomposition and soil organic matter dynamics, in: Cadisch, G., Giller, K. (Eds.), Driven by nature: plant litter quality and decomposition. CABI Publishing, Wallingford, pp. 313–335.

Philips, D.A., Fox, T.C., Six, J., 2006. Root exudation (net efflux of amino acids) may increase rhizodeposition under elevated CO_2. Global Change Biology 12, 561–567.

Reichstein, M., Katterer, T., Andren, O., Ciais, P., Schulze, E.D., Cramer, W., Papale, D., Valentini, R., 2005. Temperature sensitivity of decomposition in relation to soil organic matter pools: critique and outlook. Biogeosciences 2, 317–321.

Rumpel, C., Kogel-Knabner, I., Bruhn, F., 2002. Vertical distribution, age, and chemical composition of organic, carbon in two forest soils of different pedogenesis. Organic Geochemistry 33, 1131–1142.

Salomé, C., Nunan, N., Pouteau, V., Lerch, T.Z., Chenu, C., 2010. Carbon dynamics in topsoil and in subsoil may be controlled by different regulatory mechanisms. Global Change Biology 16, 416–426.

Sanderman, J., Baldock, J.A., Amundson, R., 2008. Dissolved organic carbon chemistry and dynamics in contrasting forest and grassland soils. Biogeochemistry 89, 181–198.

Scharpenseel, H.W., Becker-Heidmann, P., Neue, H.U., Tsutsuki, K., 1989. Bomb-carbon, ^{14}C-dating and ^{13}C-measurements as tracers of organic matter dynamics as well as of morphogenetic and turbation processes. Science of The Total Environment 81-82, 99–110.

Schimel, D.S., Braswell, B.H., Holland, E.A., McKeown, R., Ojima, D.S., Painter, T.H., Parton, W.J., Townsend, A.R., 1994. Climatic, edaphic, and biotic controls over storage and turnover of carbon in soils. Global Biogeochemical Cycles 8, 279–293.

Schrumpf, M., Schulze, E.D., Kaiser, K., Schumacher, J., 2011. How accurately can soil organic carbon stocks and stock changes be quantified by soil inventories? Biogeosciences Discussions 8, 723–769.

Søe, A.R.B., Buchmann, N., 2005. Spatial and temporal variations in soil respiration in relation to stand structure and soil parameters in an unmanaged beech forest. Tree Physiology 25, 1427–1436.

Soil Classification Working Group, 1998. The Canadian System of Soil Classification. Technical Report 1646 (Revised). Agriculture and Agri-Food Canada.

Soil Survey Division Staff, 1993. Soil survey manual. Technical Report 18. Soil Conservation Service. U.S. Department of Agriculture.

Subke, J.A., Bahn, M., 2010. On the 'temperature sensitivity' of soil respiration: Can we use the immeasurable to predict the unknown? Soil Biology and Biochemistry 42, 1653–1656.

Subke, J.A., Reichstein, M., Tenhunen, J.D., 2003. Explaining temporal variation in soil CO_2 efflux in a mature spruce forest in southern Germany. Soil

Biology and Biochemistry 35, 1467–1483.
Tarnocai, C., Canadell, J.G., Schuur, E.A.G., Kuhry, P., Mazhitova, G., Zimov, S., 2009. Soil organic carbon pools in the northern circumpolar permafrost region. Global Biogeochemical Cycles 23, GB2023.
Tonneijck, F.H., Jongmans, A.G., 2008. The influence of bioturbation on the vertical distribution of soil organic matter in volcanic ash soils: a case study in northern Ecuador. European Journal of Soil Science 59, 1063–1075.
Trumbore, S.E., 2000. Age of soil organic matter and soil respiration: Radiocarbon constraints on belowground C dynamics. Ecological Applications 10, 399–411.
Trumbore, S.E., Czimczik, C.I., 2008. An uncertain future for soil carbon. Science 321, 1455–1456.
Wheatcroft, R.A., Jumars, P.A., Smith, C.R., Nowell, A.R.M., 1990. A mechanistic view of the particulate biodiffusion coefficient: Step lengths, rest periods and transport directions. Journal of Marine Research 48, 177–207.
Wilkinson, M.T., Richards, P.J., Humphreys, G.S., 2009. Breaking ground: Pedological, geological, and ecological implications of soil bioturbation. Earth-Science Reviews 97, 257–272.
Wutzler, T., Reichstein, M., 2008. Colimitation of decomposition by substrate and decomposers - a comparison of model formulations. Biogeosciences 5, 749–759.

Appendix A. Full description of SOMPROF

Here a complete description of SOMPROF is given, including all equations. Additional explanation is given in the main text of this paper. Table A.3 gives complete overview of all symbols used in the equations. Depth (z) is assumed positive downwards and $z = 0$ is set at the top of the mineral soil. In general, subscripts suffixed to model variables denote an organic matter pool, while superscripts denote a location in the vertical profile.

Appendix A.1. Decomposition

Organic matter decomposition is modeled according to first order kinetics corrected for local soil temperature and moisture. For any organic matter pool i in model compartment p, decomposition is defined as:

$$L_i^p = f(T)\; g(W)\; k_i\, C_i^p \,, \tag{A.1}$$

where $f(T)$ and $g(W)$ are response functions for soil temperature and moisture. $f(T)$ is defined according to Lloyd and Taylor (1994):

$$f(T) = \exp\left(E_a\left(\frac{1}{T_0 - T_{ref}} - \frac{1}{T - T_{ref}}\right)\right) , \tag{A.2}$$

where T is the soil temperature (K), T_{ref} (283.15 K) and T_0 (227.13 K) are reference temperatures, and E_a (K) determines the temperature sensitivity. $g(W)$ is defined according to a modified sigmoid model (Subke et al., 2003):

$$g(W) = \exp\left(-\exp\left(a - bW\right)\right) , \tag{A.3}$$

where W is the fraction of the porosity filled with water (-) and a and b (-) are parameters determining the shape of the soil moisture response.

For several pools, part of the decomposition flux flows into to secondary pools. This is determined by the transformation factor α. The flux from pool i to pool j in model compartment p is defined as:

$$F_{i\to j}^p = \alpha_{i\to j} L_i^p \,. \tag{A.4}$$

Thus, the total formation of the secondary pools in any compartment p, is defined as follows:

$$F_{\mathrm{FL}}^p = \alpha_{\mathrm{AGL}\to\mathrm{FL}} L_{\mathrm{AGL}}^p \,, \tag{A.5}$$

$$F_{\mathrm{NLS}}^p = \alpha_{\mathrm{FL}\to\mathrm{NLS}} L_{\mathrm{FL}}^p + \alpha_{\mathrm{RL}\to\mathrm{NLS}} L_{\mathrm{RL}}^p \,, \tag{A.6}$$

$$F_{\mathrm{LS}}^p = \alpha_{\mathrm{FL}\to\mathrm{LS}} L_{\mathrm{FL}}^p + \alpha_{\mathrm{RL}\to\mathrm{LS}} L_{\mathrm{RL}}^p \,. \tag{A.7}$$

Appendix A.2. Litter input

External input of organic matter occurs for the above ground litter pool $I_{\mathrm{AGL}}^{\mathrm{L}}$ and for the root litter pool $I_{\mathrm{RL}}^{\mathrm{tot}}$. The total root litter input is distributed over the soil profile according to an exponential function of depth which starts at the top of the F horizon:

$$I_{\mathrm{RL}}(z) = I_{\mathrm{RL}}^{\mathrm{tot}}\, \beta\, \exp\left(-\beta\left(z + \Delta z^{\mathrm{F}} + \Delta z^{\mathrm{H}}\right)\right) , \tag{A.8}$$

where $I_{\mathrm{RL}}^{\mathrm{tot}}$ is the total root litter production (kg m^{-2} yr^{-1}), β (m^{-1}) is a shape parameter, and Δz^{F} and Δz^{H} are the thickness (m) of the F and H horizon, respectively, and are determined from the total mass of each layer and its bulk density:

$$\Delta z^{\mathrm{F}} = \frac{C_{\mathrm{O}}^{\mathrm{F}}}{\rho^{\mathrm{F}}} = \frac{C_{\mathrm{FL}}^{\mathrm{F}} + C_{\mathrm{RL}}^{\mathrm{F}}}{\rho^{\mathrm{F}}} \,, \tag{A.9}$$

$$\Delta z^{\mathrm{H}} = \frac{C_{\mathrm{O}}^{\mathrm{H}}}{\rho^{\mathrm{H}}} = \frac{C_{\mathrm{FL}}^{\mathrm{H}} + C_{\mathrm{RL}}^{\mathrm{H}} + C_{\mathrm{NLS}}^{\mathrm{H}}}{\rho^{\mathrm{H}}} \,. \tag{A.10}$$

The root litter input into the F and H horizon is obtained by integrating (A.8) over the horizon thickness:

$$I_{\mathrm{RL}}^{\mathrm{F}} = \int_{-\Delta z^{\mathrm{H}} - \Delta z^{\mathrm{F}}}^{-\Delta z^{\mathrm{H}}} I_{\mathrm{RL}}(z)\, \mathrm{d}z \,, \tag{A.11}$$

$$I_{\mathrm{RL}}^{\mathrm{H}} = \int_{-\Delta z^{\mathrm{H}}}^{0} I_{\mathrm{RL}}(z)\, \mathrm{d}z \,. \tag{A.12}$$

Appendix A.3. Bulk density

If mineral soil bulk density is unknown it is estimated according a function from Federer et al. (1993):

$$\rho^{\mathrm{MS}} = \frac{\rho_{\mathrm{M}}\rho_{\mathrm{O}}}{f_{\mathrm{O}}^{\mathrm{MS}}\rho_{\mathrm{M}} + (1 - f_{\mathrm{O}}^{\mathrm{MS}})\rho_{\mathrm{O}}} \,, \tag{A.13}$$

where ρ_{M} and ρ_{O} are bulk densities for hypothetical pure mineral and pure organic soil and f_{O} is the mass fraction organic matter:

$$f_{\mathrm{O}} = \frac{C_{\mathrm{O}}^{\mathrm{MS}}}{\rho^{\mathrm{MS}}} = \frac{C_{\mathrm{FL}}^{\mathrm{MS}} + C_{\mathrm{RL}}^{\mathrm{MS}} + C_{\mathrm{NLS}}^{\mathrm{MS}} + C_{\mathrm{LS}}^{\mathrm{MS}}}{\rho^{\mathrm{MS}}} \,. \tag{A.14}$$

Substituting (A.14) into (A.13) and rearranging yields:

$$f_{\mathrm{O}}^{\mathrm{MS}} = \frac{C_{\mathrm{O}}^{\mathrm{MS}}\rho_{\mathrm{O}}}{\rho_{\mathrm{O}}^{\mathrm{MS}}(C_{\mathrm{O}}^{\mathrm{MS}} + \rho_{\mathrm{M}}^{\mathrm{MS}}) - \rho_{\mathrm{M}}^{\mathrm{MS}} C_{\mathrm{O}}^{\mathrm{MS}}} \,, \tag{A.15}$$

and:

$$\rho^{\mathrm{MS}} = \frac{\rho_{\mathrm{O}}^{\mathrm{MS}}(C_{\mathrm{O}}^{\mathrm{MS}} + \rho_{\mathrm{M}}^{\mathrm{MS}}) - \rho_{\mathrm{M}}^{\mathrm{MS}} C_{\mathrm{O}}^{\mathrm{MS}}}{\rho_{\mathrm{O}}^{\mathrm{MS}}} \,. \tag{A.16}$$

Table A.3: List of symbols and abbreviations

Symbol	Description	Units
State variables and fluxes		(Organic layer / Mineral soil)
C_i^p	Content of pool i in model compartment $p^{*\dagger}$	kg m^{-2} / kg m^{-3}
I_i^p	Input of pool i in model compartment $p^{*\dagger\ddagger}$	kg m^{-2} yr^{-1} / kg m^{-3} yr^{-1}
$F_{i\to j}^p$	Transformation of pool i to pool j in model compartment $p^{*\dagger}$	kg m^{-2} yr^{-1} / kg m^{-3} yr^{-1}
F_i^p	Total formation of pool i in model compartment $p^{*\dagger}$	kg m^{-2} yr^{-1} / kg m^{-3} yr^{-1}
L_i^p	Loss of pool i by decomposition in model compartment $p^{*\dagger}$	kg m^{-2} yr^{-1} / kg m^{-3} yr^{-1}
$J_i^{p\to q}$	Bioturbation flux of pool i from model compartment p to q *†§	kg m^{-2} yr^{-1}
Model input		
k_i	Decomposition rate of pool $i^{\ddagger}$	yr^{-1}
T	Soil temperature*†‡	K
E_a	Soil temperature response parameter‡	K
W	Relative soil moisture content*†‡	-
a	Soil moisture response parameter‡	-
b	Soil moisture response parameter‡	-
$\alpha_{i\to j}$	Factor for transformation of pool i to pool $j^{\ddagger}$	-
I_{RL}^{tot}	Total root litter input in the soil profile†‡	kg m^{-2} yr^{-1}
β	Root litter distribution parameter‡	m^{-1}
B	Bioturbation rate‡	kg m^{-2} yr^{-1}
l_m	Mixing length‡	m
D_{BT}	Diffusion coefficient due to bioturbation*†	m^2 yr^{-1}
v	Advection rate‡§	m yr^{-1}
ρ^p	Bulk density in model compartment $p^{*\dagger\ddagger}$	kg m^{-3}
ρ_{M}, ρ_{O}	Pure mineral and pure organic bulk density‡	kg m^{-3}
Other variables		
z	Depth*§	m
t	Time†	yr
f_i^p	Mass fraction of organic matter pool i in model compartment $p^{*\dagger}$	-
L	Depth of the lower boundary‡	m
Model compartments (superscripts)		
L	L horizon	N/A
F	F horizon	N/A
H	H horizon	N/A
MS	Mineral soil	N/A
Organic matter pools (subscripts)		
AGL	Above ground litter	N/A
FL	Fragmented litter	N/A
RL	Root litter	N/A
NLS	Non-leachable slow OM	N/A
LS	Leachable slow OM	N/A
O	Organic matter, sum of all pools	N/A

* Depth and/or model compartment dependent
† Time dependent
‡ Input parameter
§ Positive downward

Appendix A.4. Organic matter transport

Fluxes between the organic horizons are determined by the bioturbation rate B. In case the stock in an organic horizon is zero, the bioturbation fluxes from that organic horizon are adjusted downward to the total input, if necessary, to avoid negative stocks. Thus, the bioturbation fluxes in the organic layer are defined as follows:

$$J^{\mathrm{F}\to\mathrm{H}}_{\mathrm{FL}} = \begin{cases} f^{\mathrm{F}}_{\mathrm{FL}}\, B & \text{if } C^{\mathrm{F}}_{\mathrm{FL}} > 0 \\ \min\left[\left(F^{\mathrm{L}}_{\mathrm{AGL}\to\mathrm{FL}} - L^{\mathrm{F}}_{\mathrm{FL}}\right), f^{\mathrm{F}}_{\mathrm{FL}}\, B\right] & \text{if } C^{\mathrm{F}}_{\mathrm{FL}} = 0 \end{cases}, \tag{A.17}$$

$$J^{\mathrm{F}\to\mathrm{H}}_{\mathrm{RL}} = \begin{cases} f^{\mathrm{F}}_{\mathrm{RL}}\, B & \text{if } C^{\mathrm{F}}_{\mathrm{RL}} > 0 \\ \min\left[\left(I^{\mathrm{F}}_{\mathrm{RL}} - L^{\mathrm{F}}_{\mathrm{RL}}\right), f^{\mathrm{F}}_{\mathrm{RL}}\, B\right] & \text{if } C^{\mathrm{F}}_{\mathrm{RL}} = 0 \end{cases}, \tag{A.18}$$

$$J^{\mathrm{H}\to\mathrm{MS}}_{\mathrm{FL}} = \begin{cases} f^{\mathrm{H}}_{\mathrm{FL}}\, B & \text{if } C^{\mathrm{H}}_{\mathrm{FL}} > 0 \\ \min\left[\left(J^{\mathrm{F}\to\mathrm{H}}_{\mathrm{FL}} - L^{\mathrm{H}}_{\mathrm{FL}}\right), f^{\mathrm{H}}_{\mathrm{FL}}\, B\right] & \text{if } C^{\mathrm{H}}_{\mathrm{FL}} = 0 \end{cases}, \tag{A.19}$$

$$J^{\mathrm{H}\to\mathrm{MS}}_{\mathrm{RL}} = \begin{cases} f^{\mathrm{H}}_{\mathrm{RL}}\, B & \text{if } C^{\mathrm{H}}_{\mathrm{RL}} > 0 \\ \min\left[\left(I^{\mathrm{H}}_{\mathrm{RL}} + J^{\mathrm{F}\to\mathrm{H}}_{\mathrm{RL}} - L^{\mathrm{H}}_{\mathrm{RL}}\right), f^{\mathrm{H}}_{\mathrm{RL}}\, B\right] & \text{if } C^{\mathrm{H}}_{\mathrm{RL}} = 0 \end{cases}, \tag{A.20}$$

$$J^{\mathrm{H}\to\mathrm{MS}}_{\mathrm{NLS}} = \begin{cases} f^{\mathrm{H}}_{\mathrm{NLS}}\, B & \text{if } C^{\mathrm{H}}_{\mathrm{NLS}} > 0 \\ \min\left[\left(F^{\mathrm{F}}_{\mathrm{NLS}} + F^{\mathrm{H}}_{\mathrm{NLS}} - L^{\mathrm{H}}_{\mathrm{NLS}}\right), f^{\mathrm{H}}_{\mathrm{NLS}}\, B\right] & \text{if } C^{\mathrm{H}}_{\mathrm{NLS}} = 0 \end{cases}, \tag{A.21}$$

where f^p_i is the mass fraction of pool i in compartment p:

$$f^p_i = \frac{C^p_i}{C^p_{\mathrm{O}}} = \frac{C^p_i}{C^p_{\mathrm{FL}} + C^p_{\mathrm{RL}} + C^p_{\mathrm{NLS}} + C^p_{\mathrm{LS}}}\,. \tag{A.22}$$

Note that C^p_{LS} is zero for the organic horizons. In the mineral soil, transport by bioturbation is modeled according to the diffusion equation. The transport due to bioturbation for any pool i (except above ground litter) is defined as:

$$\left.\frac{\partial C_i}{\partial t}\right|_{\mathrm{BT}} = D_{\mathrm{BT}}\frac{\partial^2 C_i}{\partial z^2}\,, \tag{A.23}$$

where the diffusion coefficient D_{BT} is defined according to:

$$D_{\mathrm{BT}} = \tfrac{1}{2}\frac{B}{\rho^{\mathrm{MS}}} l_m\,. \tag{A.24}$$

Advective transport of the LS pool in the mineral is modeled according to:

$$\left.\frac{\partial C_{\mathrm{LS}}}{\partial t}\right|_{\mathrm{adv}} = -v\,\frac{\partial C_{\mathrm{LS}}}{\partial z}\,. \tag{A.25}$$

Appendix A.5. Governing equations

Appendix A.5.1. Organic layer

The complete mass balance equations for the organic matter pools in the organic layer are as follows:

$$\frac{\partial C^{\mathrm{L}}_{\mathrm{AGL}}}{\partial t} = I^{\mathrm{L}}_{\mathrm{AGL}} - L^{\mathrm{L}}_{\mathrm{AGL}}\,, \tag{A.26}$$

$$\frac{\partial C^{\mathrm{F}}_{\mathrm{FL}}}{\partial t} = F^{\mathrm{L}}_{\mathrm{FL}} - L^{\mathrm{F}}_{\mathrm{FL}} - J^{\mathrm{F}\to\mathrm{H}}_{\mathrm{FL}}\,, \tag{A.27}$$

$$\frac{\partial C^{\mathrm{F}}_{\mathrm{RL}}}{\partial t} = I^{\mathrm{F}}_{\mathrm{RL}} - L^{\mathrm{F}}_{\mathrm{RL}} - J^{\mathrm{F}\to\mathrm{H}}_{\mathrm{RL}}\,, \tag{A.28}$$

$$\frac{\partial C^{\mathrm{H}}_{\mathrm{FL}}}{\partial t} = J^{\mathrm{F}\to\mathrm{H}}_{\mathrm{FL}} - L^{\mathrm{H}}_{\mathrm{FL}} - J^{\mathrm{H}\to\mathrm{MS}}_{\mathrm{FL}}\,, \tag{A.29}$$

$$\frac{\partial C^{\mathrm{H}}_{\mathrm{RL}}}{\partial t} = I^{\mathrm{H}}_{\mathrm{RL}} + J^{\mathrm{F}\to\mathrm{H}}_{\mathrm{RL}} - L^{\mathrm{H}}_{\mathrm{RL}} - J^{\mathrm{H}\to\mathrm{MS}}_{\mathrm{RL}}\,, \tag{A.30}$$

$$\frac{\partial C^{\mathrm{H}}_{\mathrm{NLS}}}{\partial t} = F^{\mathrm{F}}_{\mathrm{NLS}} + F^{\mathrm{H}}_{\mathrm{NLS}} - L^{\mathrm{H}}_{\mathrm{NLS}} - J^{\mathrm{H}\to\mathrm{MS}}_{\mathrm{NLS}}\,. \tag{A.31}$$

Appendix A.5.2. Mineral soil

The complete mass balance equations for the organic matter pools in the mineral soil are as follows:

$$\frac{\partial C^{\mathrm{MS}}_{\mathrm{FL}}}{\partial t} = D_{\mathrm{BT}}\frac{\partial^2 C^{\mathrm{MS}}_{\mathrm{FL}}}{\partial z^2} - L^{\mathrm{MS}}_{\mathrm{FL}}\,, \tag{A.32}$$

$$\frac{\partial C^{\mathrm{MS}}_{\mathrm{RL}}}{\partial t} = D_{\mathrm{BT}}\frac{\partial^2 C^{\mathrm{MS}}_{\mathrm{RL}}}{\partial z^2} + I^{\mathrm{MS}}_{\mathrm{RL}} - L^{\mathrm{MS}}_{\mathrm{RL}}\,, \tag{A.33}$$

$$\frac{\partial C^{\mathrm{MS}}_{\mathrm{NLS}}}{\partial t} = D_{\mathrm{BT}}\frac{\partial^2 C^{\mathrm{MS}}_{\mathrm{NLS}}}{\partial z^2} + F^{\mathrm{MS}}_{\mathrm{NLS}} - L^{\mathrm{MS}}_{\mathrm{NLS}}\,, \tag{A.34}$$

$$\frac{\partial C^{\mathrm{MS}}_{\mathrm{LS}}}{\partial t} = D_{\mathrm{BT}}\frac{\partial^2 C^{\mathrm{MS}}_{\mathrm{LS}}}{\partial z^2} - v\frac{\partial C^{\mathrm{MS}}_{\mathrm{LS}}}{\partial z} + F^{\mathrm{MS}}_{\mathrm{LS}} - L^{\mathrm{MS}}_{\mathrm{LS}}\,. \tag{A.35}$$

Appendix A.6. Boundary conditions

Appendix A.6.1. Upper boundary

The upper boundary conditions for the organic matter pools in the mineral soil are determined by the flux from the organic layer:

$$\left[-D_{\mathrm{BT}}\frac{\partial C^{\mathrm{MS}}_{\mathrm{FL}}}{\partial z}\right]_{z=0} = J^{\mathrm{H}\to\mathrm{MS}}_{\mathrm{FL}}\,, \tag{A.36}$$

$$\left[-D_{\mathrm{BT}}\frac{\partial C^{\mathrm{MS}}_{\mathrm{RL}}}{\partial z}\right]_{z=0} = J^{\mathrm{H}\to\mathrm{MS}}_{\mathrm{RL}}\,, \tag{A.37}$$

$$\left[-D_{\mathrm{BT}}\frac{\partial C^{\mathrm{MS}}_{\mathrm{NLS}}}{\partial z}\right]_{z=0} = J^{\mathrm{H}\to\mathrm{MS}}_{\mathrm{NLS}}\,. \tag{A.38}$$

Since LS-OM formed in the organic layer is assumed to flow immediately into the mineral soil, the upper boundary condition for this pool is defined as the total production in the organic layer:

$$\left[-D_{\mathrm{BT}}\frac{\partial C^{\mathrm{MS}}_{\mathrm{LS}}}{\partial z} + vC^{\mathrm{MS}}_{\mathrm{LS}}\right]_{z=0} = F^{\mathrm{F}}_{\mathrm{LS}} + F^{\mathrm{H}}_{\mathrm{LS}}\,. \tag{A.39}$$

Appendix A.6.2. Lower boundary

For all organic matter pools a zero flux boundary condition is used at depth L:

$$\left[\frac{\partial C^{\mathrm{MS}}_{\mathrm{FL}}}{\partial z}\right]_{z=L} = 0\,, \tag{A.40}$$

$$\left[\frac{\partial C^{\mathrm{MS}}_{\mathrm{RL}}}{\partial z}\right]_{z=L} = 0\,, \tag{A.41}$$

$$\left[\frac{\partial C^{\mathrm{MS}}_{\mathrm{NLS}}}{\partial z}\right]_{z=L} = 0\,, \tag{A.42}$$

$$\left[\frac{\partial C^{\mathrm{MS}}_{\mathrm{LS}}}{\partial z}\right]_{z=L} = 0\,. \tag{A.43}$$

Appendix A.7. Numerical solution

Equations (A.26-A.35) with boundary conditions (A.36-A.43) are solved numerically using finite differencing, in the order as they are listed above. The organic matter pools in the organic layer are updated using an explicit scheme, while for the mineral soil an implicit scheme, with upwind differencing for the advection term, is used.

At the end of each time step, the thickness of the mineral soil layers are updated for change of mass. For any compartment n the layer thickness updated according to:

$$\Delta z^{n,\mathrm{new}} = \Delta z^{n,\mathrm{old}} \frac{M^{n,\mathrm{new}}_{\mathrm{tot}}}{M^{n,\mathrm{old}}_{\mathrm{tot}}}\,, \tag{A.44}$$

where $M^{n,\mathrm{new}}_{\mathrm{tot}}$ and $M^{n,\mathrm{old}}_{\mathrm{tot}}$ are the total compartment mass (kg m^{-2}; mineral plus organic) for the previous and current time step, respectively. Next, the concentrations of the fractions are recalculated to assure conservation of mass:

$$C^{n,\mathrm{new}}_{i} = \frac{M^{n,\mathrm{new}}_{i}}{\Delta z^{n,\mathrm{new}}}\,. \tag{A.45}$$

Appendix B. Derivation of the diffusion equation for bioturbation

Here we derive Fick's diffusion equation from the underlying principles mixing in soils, following mixing length theory. Our derivation is based on Boudreau (1986) and Hinze (1975, ch. 1 and 5). It must be noted that the derivation is only valid under certain conditions, which are discussed in the main text of this paper, and more extensively in Boudreau (1986) and Meysman et al. (2003). Alternatively, bioturbation may be pictured as a random walk process (Meysman et al., 2003). This representation is analogous to the turbulent mixing picture presented here and also leads to the diffusion equation in the limiting case.

Bioturbation is the average effect of many short term mixing events—displacements of mass elements of the soil matrix. These mixing events are stochastic in the sense that they occur at random times and depths in the profile. Ignoring bulk density changes, we assume that the average mass displacement is isotropic, i.e. equal in all directions. Here we focus only on the vertical component of the mixing. Since a soil constituent is moved together with the soil matrix, its concentration is a stochastic variable as well. For a single mixing event, the transport of a soil constituent will be of an advective nature (not to be confused the advection caused by liquid phase transport). Material is moved at a certain rate w over a certain distance l. Hence a constituent with local concentration c is will be transported according to:

$$J = wc\,. \tag{B.1}$$

Since w and c are stochastic variables, we can apply Reynolds decomposition to split them into smooth, time-averaged components, $\overline{w}$ and $\overline{c}$, and random fluctuating components, w' and c'.

$$\begin{aligned} w &= \overline{w} + w' \\ c &= \overline{c} + c'\,. \end{aligned} \tag{B.2}$$

Substituting equation (B.2) into (B.1) yields:

$$J = \left(\overline{w}\,\overline{c} + w'\overline{c} + \overline{w}c' + w'c'\right)\,. \tag{B.3}$$

To obtain the average flux as a result of many stochastic mixing events we use time-averaging, to which applies: $\overline{\overline{p}q'} = 0$, for any two stochastic variables p and q. Furthermore, since the bioturbation process is isotropic, there is on average no net transport in any direction, i.e. $\overline{w} = 0$. Hence, the time-averaged flux is:

$$\overline{J} = \overline{w'c'}\,. \tag{B.4}$$

If the mixing distance l (which is also a stochastic quantity) is small with respect to the concentration gradient, we can approximate the fluctuation of the concentration with the first order depth derivative of $\overline{c}$:

$$c' \approx -\frac{1}{2} l' \frac{\partial \overline{c}}{\partial z}\,. \tag{B.5}$$

Substituting (B.5) into (B.4) yields:

$$\overline{J} \approx \frac{1}{2}\overline{w'l'}\frac{\partial \overline{c}}{\partial z}\,. \tag{B.6}$$

Thus, the average transport of a soil constituent is controlled by its concentration gradient and the relationship between w' and l'. In turbulent flow, $\overline{w'l'}$ specifies the combined transport by eddies of all length scales. In bioturbation, this term specifies the combined effect of mixing events over all distances. The critical assumption in mixing length theory is that most of the mixing occurs over a typical distance, the mixing length l_m, and that mixing over other distances is negligible. In that case, $\overline{w'l'}$ can be rewritten as:

$$\overline{w'l'} \approx \overline{|w'|} l_m\,, \tag{B.7}$$

where $\overline{|w'|}$ represents the average transport rate, independent of direction. $\overline{|w'|}$ is presumably directly related to the soil fauna activity If we convert the soil reworking activity B (mass area^{-1} time^{-1}) to units of volume (volume area^{-1} time^{-1}), we obtain a units of speed (length time^{-1}). Hence we propose that $\overline{|w'|}$ can be approximated by:

$$\overline{|w'|} \approx \frac{B}{\rho}\,, \tag{B.8}$$

where ρ is the bulk density of the soil matrix. Taking the divergence of (B.6) and defining a diffusion coefficient as:

$$D \equiv \frac{1}{2}\frac{B}{\rho} l_m \,, \tag{B.9}$$

we obtain the diffusion equation:

$$\frac{\partial \overline{c}}{\partial t} \approx \frac{\partial}{\partial z}\left[D \frac{\partial \overline{c}}{\partial z} \right] . \tag{B.10}$$